land

MDPI

Article

Model-Based Assessment of Giant Reed (*Arundo donax* L.) Energy Yield in the Form of Diverse Biofuels in Marginal Areas of Italy

Giovanni Alessandro Cappelli [1,*], Fabrizio Ginaldi [1], Davide Fanchini [1], Sebastiano Andrea Corinzia [2], Salvatore Luciano Cosentino [2] and Enrico Ceotto [1]

[1] CREA—AA Council for Agricultural Research and Economics, Research Centre for Agriculture and Environment, Via di Corticella 133, 40128 Bologna, Italy; fabrizio.ginaldi@crea.gov.it (F.G.); davide.fanchini@crea.gov.it (D.F.); enrico.ceotto@crea.gov.it (E.C.)

[2] Dipartimento di Agricoltura, Università Degli Studi di Catania, Alimentazione e Ambiente (Di3A), Via Valdisavoia 5, 95123 Catania, Italy; andreacorinzia89@gmail.com (S.A.C.); cosentin@unict.it (S.L.C.)

* Correspondence: giovannialessandro.cappelli@crea.gov.it

Abstract: Giant reed is a promising perennial grass providing ligno-cellulosic biomass suitable to be cultivated in marginal lands (MLs) and converted into several forms of renewable energy. This study investigates how much energy, in the form of biomethane, bioethanol, and combustible solid, can be obtained by the cultivation of this species in marginal land of two Italian regions, via the spatially explicit application of the Arungro crop model. Arungro was calibrated in both rainfed/well-irrigated systems, under non-limiting conditions for nutrient availability. The model was then linked to a georeferenced database, with data on (i) current/future climate, (ii) agro-management, (iii) soil physics/hydrology, (iv) land marginality, and (v) crop suitability to environment. Simulations were run at 500 × 500 m spatial resolution in MLs of Catania (CT, Southern Italy) and Bologna (BO, Northern Italy) provinces, characterized by contrasting pedo-climates. At field scale, Arungro explained 85% of the year-to-year variability of measured carbon accumulation in aerial biomass. At the provincial level, simulated energy yields progressively increased from bioethanol, to biomethane, and finally to combustible solid, with average values of 92-115-264 GJ ha^{-1} in BO and 105-133-304 GJ ha^{-1} in CT. Mean energy yields estimated for 2030 remained unchanged compared to the baseline, although showing large heterogeneity across the study area (changes between −6/+15% in BO and −16/+15% in CT). This study provides site-specific indications on giant reed current productions, energy yields, and natural water consumption, as well as on their future trends and stability, ready-to-use for multiple stakeholders of the agricultural sector involved in bioenergy planning.

Keywords: arungro; bioenergy planning; bioenergy yield; biomethane; bioethanol; climate change; combustible solid; crop modeling; land use; perennial energy crops

Citation: Cappelli, G.A.; Ginaldi, F.; Fanchini, D.; Corinzia, S.A.; Cosentino, S.L.; Ceotto, E. Model-Based Assessment of Giant Reed (*Arundo donax* L.) Energy Yield in the Form of Diverse Biofuels in Marginal Areas of Italy. *Land* **2021**, *10*, 548. https://doi.org/10.3390/land10060548

Academic Editors: Floortje van der Hilst, Annette Cowie and Daniela Thrän

Received: 30 March 2021
Accepted: 19 May 2021
Published: 21 May 2021

1. Introduction

In the last two decades, the governments of many countries have promoted the production and use of biofuels [1], with the aim of reducing the dependence on fossil fuels and the emission of greenhouse gases. The identification of new generation energy sources and processes minimizing the competition for land between food and energy crops is igniting the international scientific debate on sustainable energy production. The International Renewable Energy Agency [2], which is supporting countries in adopting sustainable energy pathways and regulations, identified several measures to increase bioenergy production "without competing with food production or causing land use change". In fact, when feedstock production displaces food crops in a given area, higher food price might foster the conversion of natural land into cultivation, determining an overall increase in greenhouse gas emissions. Such an undesired consequence, firstly highlighted by Searchinger et al. [3], is indicated as indirect land use change effect. In this context, the recovery of marginal lands (MLs—i.e., low-productive and profitable areas, which tend to be abandoned [4]) to plant permanent, non-food and low-input species is emerging as a valid option to produce low-cost renewable energy and preserve environmental sustainability.

In addition to natural constraints on crop productivity, projected negative effects of climate change on yield stability and crop productivity are expected to further penalize the cultivation of traditional crops in MLs in the short-term, especially in Mediterranean areas under no adaptation [5,6]. As a consequence, a larger quantity of agronomic inputs will be presumably needed to reduce projected yield losses due to the increasing occurrence of heat stress and drought during crucial phenological phases, such as around flowering and pollination [7,8]. The increased request of inputs will likely cause an increment of production costs, especially intensifying the competition between rural and urban areas for water use during summer [9,10]. Within this framework, new supply chains and processes have been developed and tested worldwide at lab and/or small scale in order to reduce the fossil fuel dependency through a responsible use of resources, while preserving the income of stakeholders of the energy sector [11–15].

Among non-food energy species, giant reed (*Arundo donax* L.) is a low-input, high-yielding, rhizomatous perennial grass, well-adapted to a variety of pedo-climatic conditions and suitable as feedstock for the production of biofuels/bioenergy via biological fermentation (i.e., bioethanol and biogas) and/or direct biomass combustion [16–18]. As a matter of fact, in Southern European climates, this crop can be grown in many soils, ranging from heavy clay to loose sands and gravel soils, and also tolerates both high salinity and extended periods of drought [19]. Besides its rusticity, this species can provide several ecosystems services: an outstanding biomass productivity [20]; a substantial soil carbon sequestration [21]; high nitrogen (N) use efficiency [22]; and an effective residual soil nitrate removal across soil profile [23]. Furthermore, the very deep root system allows the crop to adsorb soil pollutants, favoring soil phytoremediation and aggregation [10]. Thanks to the advantageous balance between biomass yield, fiber composition and amount and cost of agronomic inputs needed to grow the crop under unstressed conditions, giant reed, as a second-generation energy source, demonstrated to provide higher energy yield per hectare compared to conventional crops also in Mediterranean and Italian environments [17,24,25]. Corno et al. [24] reported that giant reed produces on average 11,000 L ha^{-1} of bioethanol, which is approximately 1.25 times more than the yield obtainable from miscanthus, 1.8 times more than sugar cane and sugar beet, and 3.7 times more than corn and sweet sorghum. Although fermentation-based pretreatments are generally needed to facilitate the hydrolysis of lignocellulosic materials for bioethanol production, the second-generation bioethanol presents advantages that are mainly related to the high biofuel yield per surface unit, the positive energy balance, and the negative greenhouse gas emissions [26]. As regards biogas production, giant reed is characterized by a lower anaerobic bio-gasification potential compared to conventional crops (i.e., corn, sorghum and rye) because of the absence of aboveground storage organs containing high-energy compounds such as starch [24]. Nevertheless, the high biomass productivity allows to obtain higher biomethane production per hectare compared to other energy crops, especially when a single annual harvest at the end of the growing season is adopted [25]. Although the crop biomass does not require any fermentation pretreatment when it is harvested within a range of dry matter content between 30 and 38% [27], a recent study showed that a thermo-chemical pre-treatment with KOH at 120 °C was able to increase the methane yield by about 20%, while reducing the anaerobic digestion duration by about 10 days [28]. Given the high biomass productivity and the high heating value (HHV; 18.7 MJ kg^{-1} according to Danelli et al. [29]), the crop also shows a promising potential for direct combustion, even though it has high ash content, coming from leaf tissues, which can reduce thermal conversion efficiency especially in the early season harvesting. The average HHV ranges between 17.5 and 19.9 MJ kg^{-1} [24,30] and is very similar to that of woody biomass (e.g., poplar, 19.3 < HHV < 19.7 MJ kg^{-1}) and other herbaceous species such as miscanthus (17.8 < HHV < 19.6 MJ kg^{-1}) and switchgrass (17.8 < HHV < 19.6 MJ kg^{-1}) [24].

In this context, biophysical models represent a cost-effective solution and are commonly used to perform integrated a priori evaluations of crop response across different environments and management practices, under both current and climate change scenarios [31]. Recent model-based studies revealed that biomass productivity of giant reed grown under non-limiting water and nitrogen conditions is expected to rise in the future, in both lowlands [27] and marginal wetlands around riverbeds in Northern Italy [10,18,32]. However, the evaluation of climate change impact on giant reed productivity under rainfed condition [33] and on its energy potential in terms of biomethane, bioethanol, and thermal energy production is still an open issue, in spite of the crucial implications for mid-term planning policies. In fact, to date, no research studies are available in the literature that couple models for the dynamic simulation of giant reed growth/yield as driven by pedo-climatic and management conditions (e.g., cutting time) with algorithms quantifying the potential of crop-derived substrates for bioenergy production, neither point nor large-scale. This combination represents an innovative tool in supporting bioenergy planning, which is very useful for the recovery and enhancement of marginal lands, especially from a climate change perspective. As a matter of fact, the growing demand for energy and the concurrent projected energy shortage in the near future, require innovative planning strategies to minimize the increasing gap between energy demand and supply [34].

In this context, the goal of this study was an extensive spatially explicit analysis of future trends of giant reed obtainable biomethane, bioethanol, and combustible solid in MLs of Italy in the short term.

2. Materials and Methods

This exploratory study was performed via the application of the biophysical Arungro model (rainfed conditions; [35]) at 500 m spatial resolution by combining the latest generation of crop growth models; climate change scenarios from the Intergovernmental Panel on Climate Change (IPCC); and databases with in-depth information on soil chemical/physical characteristics, marginality, and crop suitability to environment. The analysis was centered on the Catania and Bologna provinces, which are characterized by contrasting pedo-climatic conditions and well represented in terms of calibration dataset. This choice was closely connected to the purposes of the study, which intends to provide policy makers with useful information to consolidate (e.g., Bologna) or expand (e.g., Catania) the bioenergy sector in a sustainable way, by enhancing national marginal areas. In this context, Bologna is located in the heart of the main Italian district where a large scale biogas supply chain has been developed and consolidated, over the last two decades, due to European Directives on Nitrates (EEC, 1991) and the Renewable Energy (EC, 2009/28/EC, 2009). Catania is characterized by a multitude of abandoned marginal areas, where giant reed grows well in the absence of water and nitrogen supply. The abovementioned considerations and the growing interest from the public and private sector in launching new funding resources/projects in the province Catania emerges as an interesting investment opportunity in the medium and long term, which deserves to be explored in addition to Bologna.

2.1. Study Area and Bionergy Sector Maturity

The analysis was centered on the Italian provinces of Catania (Southern Italy) and Bologna (Northern Italy; Figure 1), which are characterized by contrasting pedo-climatic conditions, giant reed productivity, and prospects in terms of development of the bioenergy sector.

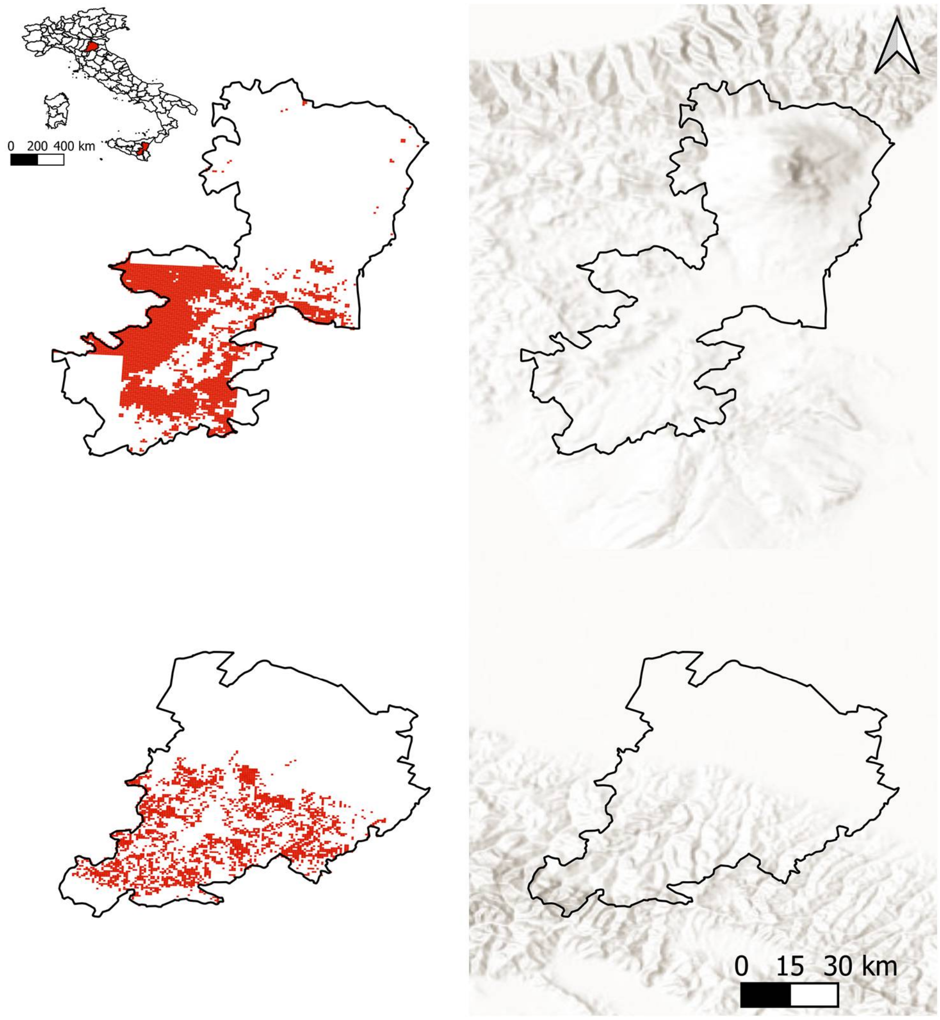

Figure 1. Marginal areas (in red) of Catania (**top panels**) and Bologna (**bottom panels**) provinces and related elevation maps (**right side**).

The Catania province (CT, Sicily region) accounts for a total ML area of 1126.6 km^2. According to the Köppen–Geiger taxonomy [36], the climate in the area is Mediterranean, with a mean annual temperature of 17.8 °C and a dry hot summer (i.e., maximum temperature frequently exceeds 30–35 °C in July and August). Average cumulative annual rainfall is 567 mm, with a main rainy period in winter. Soil texture widely varies across the province, including silty loam, clay, sandy loam, loamy sand, and sandy clay loam soils. Giant reed productivity ranges between 42 and 47 Mg ha^{-1} and between 31 and 38 Mg ha^{-1} under well-irrigated and rainfed conditions respectively [33,37]. The Bologna province (BO, Emilia Romagna region) contains an overall ML area of 880 km^2. The climate in the region is temperate sub-continental, characterized by relatively high temperatures and evenly distributed precipitation throughout the year [25]. Average annual air temperature is about 13 °C, fluctuating from 0 to 5 °C in winter months, to peaks over 30 °C in the period June–August. Total annual precipitation is in the range of 700–900 mm, with two main rainy periods in spring and fall and a minimum in June–August. Soil texture mainly consists of silty loam and clay soils, with relatively high water-holding capacity. Giant reed productivity ranges between 41.5 and 61 Mg ha^{-1} under non-limiting conditions for water availability, whereas rainfed productions fluctuated between 20 and 30 Mg ha^{-1} [33].

A more detailed characterization of the pedo-climatic variability across MLs is presented in Figure 2. Data shown confirm the choice of the two provinces, which present very contrasting soil and weather conditions: the Catania province is characterized by higher temperatures and much drier spring-summer periods compared to Bologna, and shows much more superficial soils, richer in organic matter and silt, but with less sand and clay content.

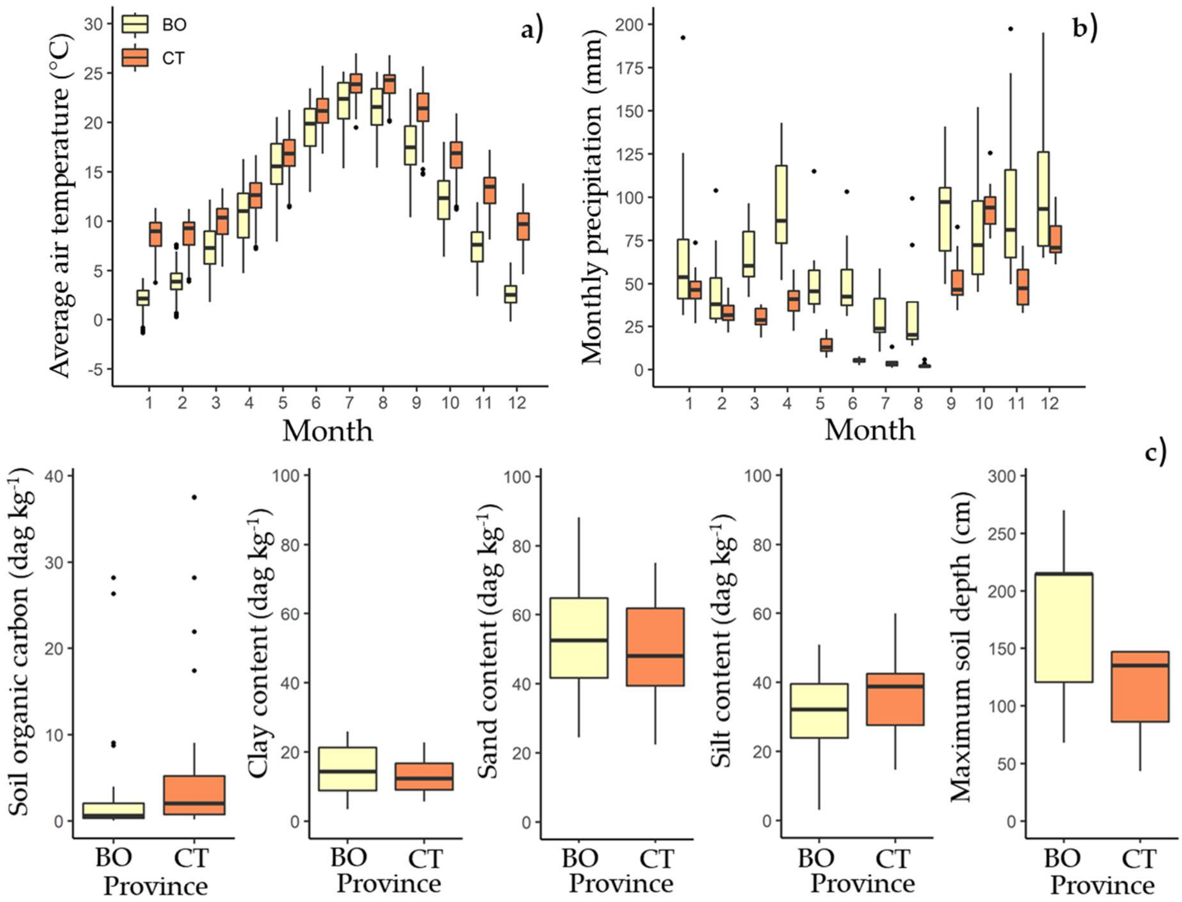

Figure 2. Pedo-climatic characterization of Bologna (BO) and Catania (CT) provinces under current climate conditions. (**a**,**b**) Mean trends of monthly average air temperature and monthly precipitation during the period 1993–2007 for all the marginal lands (MLs) considered in the spatially distributed simulation experiment (Section 2.3). (**c**) Variability of the main soil characteristics across MLs. Black dots represent outlier values.

Concerning renewable energy production, in Italy there are 1681 biogas plants throughout the country, of which there are 762 for electricity production and 919 for the combined production of electricity and heat [38]. Seventy-five percent of materials used to feed the biogas plants derive from agriculture, whereas the remaining 25% are from municipal wastes. In this context, while Emilia-Romagna accounts for 252 biogas plants and 6 for biomethane production, in Sicily there are only 14 biogas plants and none producing biomethane [39].

Conversely, dedicated projects for the production of second-generation bioethanol have started only recently and involve both public and private branches of the energy sector. In this context, the first commercial plant in Europe was commissioned by Beta Renewables in 2013 at Crescentino (Vercelli, Northern Italy) with a capacity of 40.000 Mg year^{-1} of bioethanol [40]. In 2014, the collaborative project COMETHA (http://www.cometha.eu/; accessed on 19 May 2021) was launched to develop an industrial scale pre-commercial plant for second generation bioethanol and other co-products from lignocellulosic feedstock in Porto Marghera (Venezia, Northern Italy).

2.2. Model Description and Calibration

The Arungro model [35] was used for the simulation of giant reed development and growth, considering soil water balance and agricultural practices (i.e., transplanting and cutting times). Arungro simulates daily net carbon fixation as a balance between gross photosynthesis and growth/maintenance respiration, depending on radiation interception and crop transpiration. The model implements a detailed description of leaf area index dynamics at shoot and plant levels, accounting for leaf size heterogeneity on a single stem and among stem cohorts. The evolution of stem number is simulated based on thermal time, with the emission of new tillers regulated by rhizome biomass during sprouting. The water stress limitation to gross photosynthesis rate was simulated by a stress function (0–1, 1 = no stress) based on the ratio between actual root water uptake and crop demand. Root water uptake was computed according to potential evapotranspiration demand, soil water content, and root depth, based on the Environmental Policy Integrated Climate (EPIC) model [41]. Soil water redistribution was described with a tipping-bucket approach [42], assuming that water can flow to downward soil layers when the field capacity of the above layers is exceeded.

Model parameters were calibrated in a preliminary study [33] and were applied herein to reproduce the dynamics of carbon accumulation in the aerial biomass (CAAB; Mg C ha^{-1}); in that paper, the model was trained using multi-year experimental datasets including in-season measurements of aboveground biomass and leaf area index collected in six locations across Italy in the period 1997–2013, in both rainfed and irrigated systems, under non-limiting conditions for nitrogen availability. To the scope, CAAB was derived according to raw material composition of giant reed dry matter [43]. Model performances were quantified using standard metrics in crop modeling studies, as relative root mean square error (RRMSE, minimum and optimum = 0%; maximum = +∞, Ref. [44]), coefficient of residual mass (CRM, minimum = $-\infty$, maximum = +∞, optimum = 0, unitless, Ref. [45]; if positive indicates model underestimation and vice versa) and the modelling efficiency (EF, minimum = $-\infty$, optimum and maximum = 1, unitless, Ref. [46]; if positive, the model is a better predictor than the mean of measured values and results can be considered acceptable, Ref. [47]). This activity laid the foundation to the spatially distributed simulation experiment, in which biomethane, bioethanol, and combustion yield from giant reed biomass were estimated across MLs of Italy.

2.3. Spatially Distributed Simulation

The Arungro model was linked to a georeferenced database with information on current and future climate scenarios, crop management, soil properties, land marginality, and crop suitability to different environments (Figure 3).

Daily downscaled weather data (0.25° spatial resolution) for current and future climate conditions were borrowed from Duveiller et al. [48], who generated 30-year bias-corrected synthetic series for three divergent realizations of the same IPCC emission scenario (A1B, provided by the IPCC's Fourth Assessment Report): DMI-HIRHAM5-ECHAM5, ETHZ-CLM-HadCM3Q0, and METOHC-HadRM3Q0-HadCM3Q0. ETHZ−CLM−HadCM3Q0 was chosen as the reference climate change scenario, since representing the intermediate projection of A1B scenario among the three available (i.e., mean temperature raises up to 1.4 °C and mean decrease in cumulative precipitation up to -30% in the period April–September). Time series centered on near past (2000) and near future (2030) were considered.

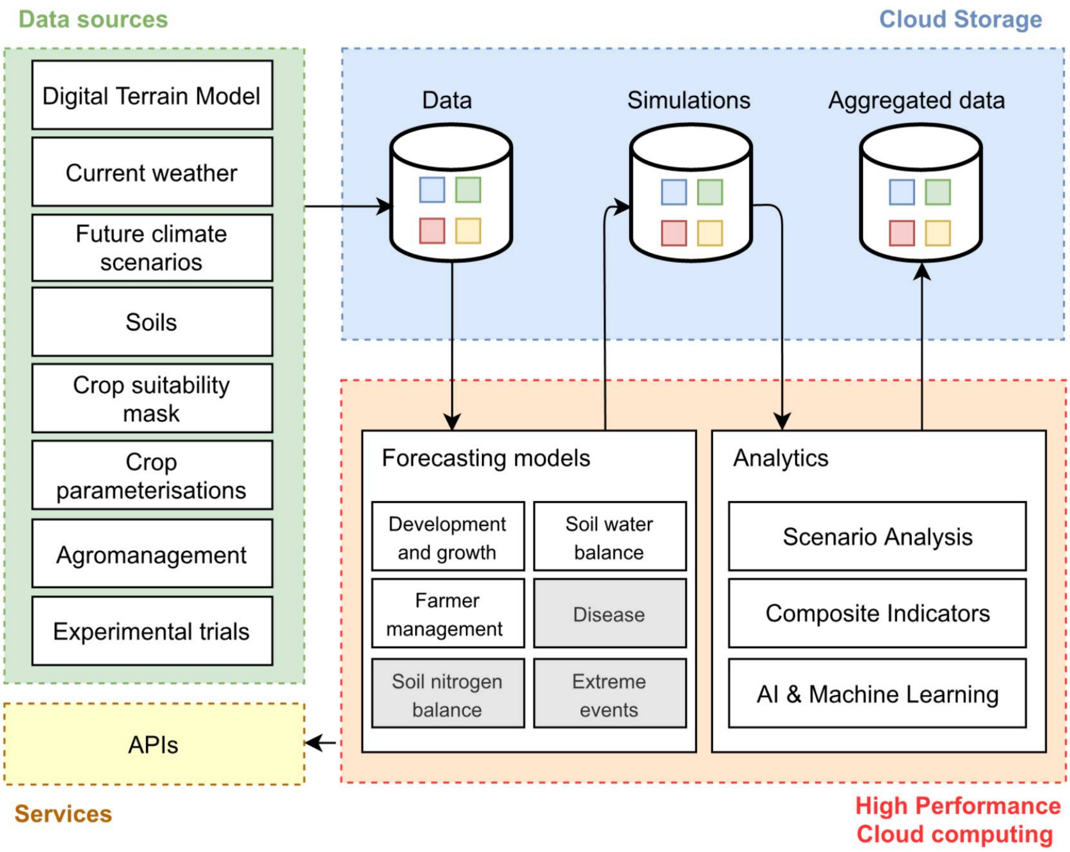

Figure 3. Schematic representation of the simulation environment developed for the AGROENER project (http://agroener.crea.gov.it/; accessed on 19 May 2019). Processes indicated in grey boxes were not considered in the present study.

Soil hydraulic properties, necessary to parametrize the soil water module, were derived on the fly, via pedo-transfer functions [49], by soil texture and organic matter data available at 500 × 500 m resolution across Italy [50]. Texture data were considered within the rooting soil depth, i.e., soil profile without physical constraints to root deepening.

Maps of soil marginality and crop suitability were built at 250 m spatial resolution in the framework of the AGROENER project [4,51]. MLs were defined as non-protected areas, without natural constraints to productivity and an average value of agricultural land (AVAL) lower than the average regional AVAL. Three classes of marginality were defined: (i) high (<30% of AVAL), intermediate (30–60% of AVAL), and low (60–99% of the AVAL). Land suitability was assessed via a fuzzy Multi-Criteria Analysis based on multiple environmental factors: (i) climatic (annual mean air temperature and total rainfall, absolute minimum air temperature), (ii) topographic (distance from the sea coast, slope), and (iii) pedological (soil texture and depth). Each factor was scored based on its suitability for giant reed cultivation and scores were then aggregated in a final suitability index ranging from 0 (no suitable) to 1 (complete suitability). Three classes of suitability were defined: (i) suitable land (score = 0.90–1.00); (ii) marginally suitable land (score = 0.70–0.89); and (iii) low suitable land (score = 0.00–0.699).

Site-specific transplanting data were derived from literature and expert knowledge. Harvest was set at the end of November—i.e., before leaf senescence.

Soil grid-cell was defined as simulation unit (SU) and information layers were univocally assigned to each SU on the basis of spatial attributes (i.e., geographic coordinates of centroids), via the use of GIS (geographic information system) applications according to Ginaldi et al. [31]. A total of 5991 SUs was defined in the study area (4765 in the province of Catania and 1226 in Bologna, respectively), excluding low marginality and low/intermediate suitability classes. Simulations were performed for every possible combination between IPCC emission scenario (1) × realization (1) × time frame (2) × year (30) × grid cell (5992) under water-limited conditions, for a total of 359,520 years simulated.

2.4. Software Infrastructure

The BioMA modelling framework (Biophysical Model Applications; https://en.wikipedia.org/wiki/BioMA; accessed on 19 May 2019), which is a software platform designed to develop, run, and test mathematical models on generic spatial units in the domains of agriculture and environmental science, provided the infrastructure to retrieve input data and perform simulations (Figure 3). Within this framework, the cropping system is segregated into different domain-specific compartments (e.g., crop, soil, farming practices, . . .), which are codified, separately, as independent software units called components. Model components can be then inter-linked into more complex simulation chains aimed at specific modelling goals (modelling solutions—MSs) and coupled with a spatially explicit database with information on climate, crop distribution, and soil properties. The MS handles the simulation time and the call order of the simulation components within a time step. The MSs can be run via a sample console application, in BioMA applications (e.g., BioMA-Site, BioMA-Spatial, Optimizer, etc), via a dedicated adapter, or can be called online via a RESTful API (application program interface) request. In the framework of the AGROENER project (http://agroener.crea.gov.it/), the BioMA tools have been modified and used in a "Software as a Service" (SaaS) perspective, i.e., a software licensing and delivery model in which software is licensed on a subscription basis and is centrally hosted. This concept was grounded on the Microsoft Azure Functions, which are tools specifically designed to provide stateless functionalities that respond to a RESTful call (https://en.wikipedia.org/wiki/Representational_state_transfer; accessed on 19 May 2019). This concept agrees well with the requirements of the BioMA platform, in which a model can be run independently from one simulation unit to another (i.e., no interactions among simulation units are considered). The response to the single call to the Azure Function [52] is processed in the Microsoft Azure cloud; both the call and the answer take the shape of an http call (and its response) and are therefore immediately available on the web. To log in, the user should provide a personal token, which is released upon registration. At last, the built-in features of the Azure cloud allowed for a high degree of parallelization of model simulations, due to the massive data processing. Details of the call to the RESTful API of the Arungro model are documented in the Supplementary Materials (Text S1).

2.5. Analysis of Results

Outputs achieved in model calibration were used to plot simulated daily dynamics of CAAB versus observed data, differentiating by location and water regime (fully irrigated vs. rainfed).

The outputs of 30-year spatially explicit simulations were used to describe the overall variability of CAAB, biomethane (Nm^3 ha^{-1}), and bioethanol (L ha^{-1}) productions in the form of a table, as well as the energy yield that may be achieved from the combustion of these substrates in the baseline and 2030 via the use of boxplots. Biomethane, bioethanol, and energy yields were derived combining simulated values of above ground biomass (Mg ha^{-1}) and potential biomethane (275.6 Nm^3 CH_4 Mg^{-1} DM, computed by averaging experimental data reported by Di Girolamo et al. [53,54]; Corno et al. [24]; Yang and Li [55], Liu et al. [56]; Jiang et al. [57]; Shilpi et al. [58] Ceotto et al. [25]; Vasmara et al. [28]) and bioethanol (217.7 L Mg^{-1} DM, computed by averaging experimental data reported by Bura et al. [59]; Scordia et al., [60]; Corno et al. [24]; and Viola et al. [61]). The efficiency with which the crop biomass is converted to biomethane is referred to as specific methane yield (SMY) and expressed as mL CH_4 g^{-1} VS (volatile solids, i.e., DM minus ash content), in standard conditions (STP) of temperature (273.15 K) and pressure (101.3 kPa). For giant reed harvested in October, the ash content is about 5% [25], but its content is decidedly much higher for summer harvest (6.59–8.32%), due to the higher fraction of leaves in total biomass. The values reported above were then used to calculate the energy production per surface unit obtainable from biomethane (234 GJ ha^{-1}; plant efficiency of 80.8%. and LHV of 31.6 MJ m^{-3}), bioethanol (186 GJ ha^{-1}; CH_3CH_2OH density of 788 kg m^{-3} and LHV of 26.8 MJ kg^{-1}), and combustible solid (536 GJ ha^{-1}; water specific heat of 4.18 kJ kg^{-1} K^{-1} in the range of temperature 297.15–373.15 K, water latent heat of vaporization 2.27 MJ kg^{-1} and LHV of 16.8 MJ kg^{-1}), considering an average dry biomass production of 37.7 Mg ha^{-1} and a moisture content of 50% (i.e., 37.7 Mg ha^{-1}). In Italian conditions, giant reed is generally harvested in October–November with a moisture content of about 50–55%. Indeed, while late harvests allow exploiting radiative and thermal benefits during the summer and realizing top yield performances even under rainfed conditions, summer cuts provide much lower yield and require dedicated pre-treatments to reduce the higher moisture content at harvest (i.e., 70–75%, Ref. [25]). The energy yield values computed for combustion were in line with experimental data reported by Angelini et al. [62] and Bracco et al. [63], who obtained values in the range of 410–592 GJ ha^{-1} for a giant reed crop grown under non-limiting conditions for nutrients availability, starting computation from the second year after crop establishment. Furthermore, results were averaged on each simulation unit, considering each combination emission scenario × climate realization × time frame, and then used to (i) inspect the spatial variability of bioethanol, biomethane, and combustion under current climate and (ii) assess the impact of climate change as percentage difference compared to the baseline. Percentage variation in terms of water requirement was also computed based on actual crop evapotranspiration. Finally, the coefficient of variation (CV) was used to explore the within-cell variability of energy yields in both time frames.

3. Results

3.1. Calibration

The values of Arungro parameters after calibration are reported in Table 1, together with their biophysical range of variation, unit of measurement, and description. Forty-one parameters were calibrated, while 24 were left at the default value, according to model documentation. A single set of parameters was developed for both locations. Maximum tiller population (MaxTillerPop, ID 43, Table 1) mirrors transplanting density in experimental trials (Bologna, 2.78 rhizomes m^{-2} and Catania, 2.5 rhizomes m^{-2}), while considering the same number of attainable culms per rhizome (11.2).

Table 1. Arungro parameter list. Parameter values marked with "D" were set to defaults, while the remaining ones ("C") were calibrated within ranges reported in model documentation. BO = Bologna; CT = Catania.

ID	Parameter	Description	Unit	Max	Min	Value	Source
1	BaseRootBiomForTillerDev	Minimum root biomass value for tiller development	°C	5	0	0	D
2	BaseTempForConvEff	Base temperature for conversion efficiency	°C	25	0	8.30	C
3	BaseTempForEmerg	Base temperature for emergence from planting or ratooning	°C	30	0	2.94	C
4	BaseTempForLeafEm	Base temperature for leaf emission	°C	25	5	6.44	C
5	BaseTempForPhotos	Base temperature for photosynthesis	°C	20	0	6.59	C
6	BaseTempForPlantExt	Base temperature for plant extension	°C	20	5	5.52	C
7	BaseTempForRootExt	Base temperature for root extension	°C	30	0	10	D
8	BaseTempForStalkElo	Base temperature for stalk elongation	°C	16	0	9.36	C
9	BaseTempForTillerDev	Base temperature for tiller population development	°C	20	10	10.32	C
10	CropCoefficient	Crop coefficient	-	10	0	1.15	D
11	CutOffTempForLeafEm	Cutoff temperature for leaf emission	°C	50	25	36.14	C
12	CutOffTempForRootExt	Maximum temperature for root extension	°C	40	25	30.96	C
13	CutOffTempForStalkElo	Cutoff temperature for stalk elongation	°C	40	25	40	C
14	CutOffTempForTillerDev	Cutoff temperature for tiller population development	°C	40	25	29.13	C
15	FractionOfDyingTiller	Fraction of tillers above the future mature tiller population (at 1600 °Cd) that senesce per unit thermal time	(°Cd)$^{-1}$	0.005	0.003	0.0024	C
16	FractGrossPhotoGroResp	Fraction of gross photosynthesis lost for growth respiration	-	1	0	0.18	C
17	FracPlantEloDueToStalkElo	Fraction of plant elongation attributable to stalk elongation	-	1	0	0.45	D

Table 1. *Cont.*

ID	Parameter	Description	Unit	Max	Min	Value	Source
18	LeafAngle	Leaf angle	°	90	0	25	D
19	LeafIDForLeafAreaLimit	Leaf ID above which leaf area is limited	-	40	0	15	D
20	LeafNumAtPhylloSwitch	Leaf number at which the phyllocron changes	-	500	0	18	D
21	LeafNumForMaxLightExt	Leaf number at which maximum light extinction occurs	-	100	0	20	D
22	MaxRadConvEff	Maximum radiation conversion efficiency	g MJ^{-1}	20	0	9.98	C
23	MaxCanopyLightExtCoeff	Maximum canopy light extinction coefficient	-	1	0	0.84	C
24	MaxLeafArea	Maximum leaf area assigned to all leaves above LeafIDForLeafAreaLimit	cm^2	650	50	354.71	C
25	MaxLeafLength	Absolute maximum leaf length	cm	110	50	52.53	C
26	MaxLeafWidth	Absolute maximum leaf width	cm	10	1	3.87	C
27	MaxNumExpLeaves	Maximum number of expanding leaves on a tiller	-	40	0	7	C
28	MaxNumWellWaterGrLeaves	Maximum number of green leaves under well water conditions	-	50	0	30	C
29	MaxNumberOfLeavesPerTiller	Maximum number of leaves per tiller	-	40	1	37	C
30	MaxPartFractToAerialDryMass	Maximum partition fraction to aerial dry mass	t t^{-1}	1	0	0.85	C
31	MaxRootBiomForTillerDev	Maximum root biomass for tiller development	°C	30	0	20	D
32	MaxTempForConvEff	Maximum temperature for conversion efficiency	°C	40	0	32.38	C
33	MaxLeafArea1	Cultivar parameter for quadratic equation for max leaf area	cm^2	10	−10	0	D
34	MaxLeafArea2	Cultivar parameter for quadratic equation for max leaf area	cm^2	100	−10	0	D
35	MaxLeafArea3	Cultivar parameter for quadratic equation for max leaf area	cm^2	300	−50	180	D
36	MaxLeafLengthPerLeafN1	Parameter for quadratic equation for max leaf length per leaf number	cm	10	−10	0	D
37	MaxLeafLengthPerLeafN2	Parameter for quadratic equation for max leaf length per leaf number	cm	30	−10	0	D
38	MaxLeafLengthPerLeafN3	Parameter for quadratic equation for max leaf length per leaf number	cm	120	−10	65	D
39	MaxLeafWidthPerLeafN1	Parameter for quadratic equation for max leaf width per leaf number	mm	5	−5	0	D
40	MaxLeafWidthPerLeafN2	Parameter for quadratic equation for max leaf width per leaf number	mm	5	−5	0	D
41	MaxLeafWidthPerLeafN3	Parameter for quadratic equation for max leaf width per leaf number	mm	120	−10	60	D
42	MaxRootLengthDensity	Maximum root length density	cm cm^{-3}	50	0	4.82	C
43	MaxTillerPop	Maximum tiller population	tiller m^{-2}	50	15	31^{BO}; 28^{CT}	C
44	MinCanopyExtinctionCoeff	Minimum canopy extinction coefficient	-	1	0	0.57	C
45	MinPartFractAerialDryMass	Minimum partition fraction to aerial dry mass	t t^{-1}	1	0	0.086	C
46	MinRootLengthDensity	Minimum root length density	cm cm^{-3}	50	0	0.02	D
47	OptRootBioForTillerDev	Optimum root biomass for tiller development	°C	20	0	10	D
48	OptTempForConvEff	Optimum temperature for conversion efficiency	°C	30	0	18.39	C
49	OptTempForEmergence	Optimum temperature for emergence from planting or ratooning	°C	45	15	31.95	C
50	PartFractionAtHighTemp	Fraction of aerial dry mass partitioned to stalk at high temperature	t t^{-1}	1	0	0.76	C
51	PartCoefficient	Partitioning Coefficient for aerial dry mass	-	1	0	0.558	C
52	PhylloInterAboveSwitchN	Phyllocron interval 2 (for leaf numbers below Pswitch,°C.d (base TTBASELFEX))	°Cd	500	0	90	D
53	PhylloInterBelowSwitchN	Phyllocron interval 1 (for leaf numbers below Pswitch,°C.d (base TTBASELFEX))	°Cd	500	0	40	D
54	Q10ForMaintenanceResp	Fractional increase in respiration rate per 10°C rise in temperature	-	5	0	1.68	D
55	ReferenceMaintenanceResp	Value of maintenance respiration at 10 °C	t t^{-1} d^{-1}	1	0	0.004	C
56	RootDepthIncrPerGDD	Root depth increase per growing degree day	cm $(°Cd)^{-1}$	0.5	0	0.1	C
57	RootLengthPerMassOfRoot	Root length per mass of root	cm g^{-1}	10,000	0	500	D
58	SoilWaterSupplyPotETCoeff1	Soil water supply potential ET ratio. Thershold below which evaporation and photosynthesis are limited	-	10	0	0.016	C
59	SoilWaterSupplyPotETCoeff2	Soil water supply potential evapotranspiration ratio. Thershold below which expansive growth is limited	-	10	0	1	C
60	ThermTimeForStalkElo	Thermal time after which stalk elongates	°C	1800	800	1015.89	C
61	ThermTimeToEmergFromPlant	Thermal time to emergence for a plant crop	°Cd	900	10	14.81	C
62	ThermTimeToEmergFromRatooning	Thermal time to emergence for a ratoon crop	°Cd	500	0	15	C
63	TillerPopulationAfter1600TT	Tiller population after 1600 thermal time	tiller m^{-2}	30	1	13.39	C
64	TTEmergenceToPeakTillerPop	Thermal time emergence to peak tiller population	°Cd	900	300	632.8	C
65	UnstressedPlantExtensionRate	Unstressed plant extension rate	mm $°C^{-1}h^{-1}$	5	0	0.215	C

The daily dynamics of CAAB (Mg C ha^{-1}) simulated at field level in model calibration are presented in Figure 4, together with the values of the statistical metrics of agreement between reference and simulated data.

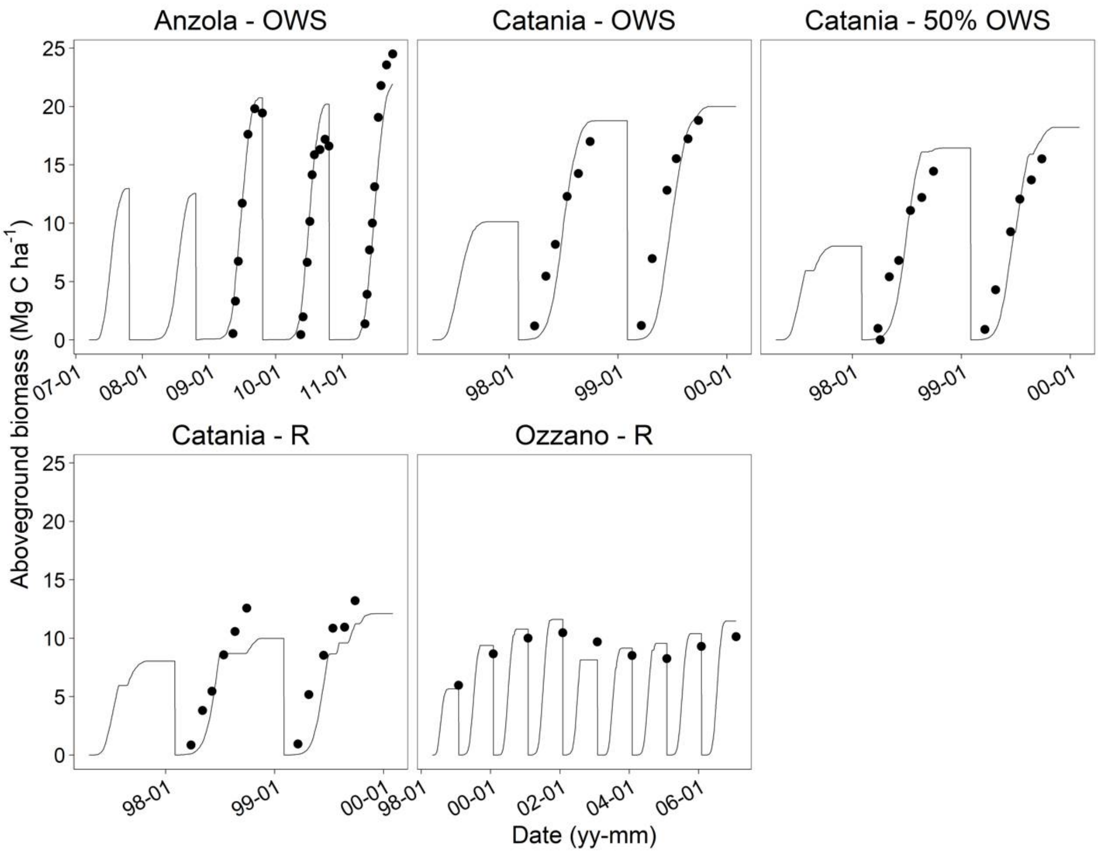

Figure 4. Model performances in reproducing the dynamics of carbon accumulation in aerial biomass (CAAB, black line) during the vegetative season of giant reed. Measurements of CAAB (black dots) were collected in three experimental sites in the 1997–2013 period, from plots with (R = rainfed) and without (OWS = optimum water supply) water stress and with different combinations of stand densities and harvest times. Anzola and Ozzano are located in the province of Bologna (Northern Italy), whereas Catania is situated in the province of the same name (Southern Italy). In BO, abundant precipitation (annual mean of 840 $\pm$ 40 mm) and high soil water retention capacity under current conditions are enough to ensure potential conditions for water availability, preventing irrigation treatments during growing seasons. Conversely, in the CT province, a total of about 400 mm of irrigation water was applied during each growing season in order to avoid crop water stress, given the low precipitation and high temperature during the April–September period.

Arungro accurately reproduced the evolution of CAAB along the growing season in all the experiments, with an average RMSE of 2.04 Mg ha^{-1} (RRMSE = 27.96%) and explaining the 85% of the inter-annual variability (EF = 0.81). Larger errors corresponded to the second year experiment in CT (Catania—R), in which the average underestimation of CAAB was about 3.2 Mg C ha^{-1}. CRM values showed a slight systematic underestimation of CAAB (CRM = 0.11), especially at mid and late vegetative stages, due to a slight delay in the simulated dynamics of tiller number and leaf development over the vegetative season. Furthermore, the onset of leaf senescence started earlier in simulations compared to field observations. In CT, Arungro properly simulated the dependence of CAAB from water availability, with a marked CAAB decline from full (i.e., 100% ET restitution) to medium (i.e., 50% ET restitution) and no irrigation treatments (i.e., 0% ET restitution). Arungro correctly simulated CAAB values obtained in experimental sites of BO province, with a rising trend from rainfed (Ozzano) to potential conditions for water availability (Anzola). Although field trials were performed on soils with similar textures, the weather data in Anzola were characterized by very favorable precipitation during giant reed growing season (average of 632 mm compared instead of 440 mm in Ozzano) and more advantageous thermal regimes for development and growth (mean temperature of 15.1 °C compared to14.7 °C in Ozzano).

3.2. Spatially Distributed Simulations

The average values of simulated CAAB, biomethane (Nm^3 ha^{-1}), and bioethanol (L ha^{-1}) in baseline and 2030 for BO and CT provinces are reported in Table 2, together with standard deviation. Biomass and biofuel productions simulated in CT were always higher and more variable with respect to those achieved in BO, regardless of the time frame considered. For the baseline scenario, average simulated CAAB were approximately 7.5 Mg C ha^{-1} in CT and 8.5 Mg C ha^{-1} in BO, with differences due to soil variability overcoming those resulting from weather conditions (the within-province weather conditions were very homogeneous compared to the pedological ones, due to the rougher spatial resolution of available data). Average CAAB simulated in 2030 and related variability were almost unchanged when compared with the baseline, with average values of 7.4 Mg C ha^{-1} in BO and 8.6 Mg C ha^{-1} in CT.

Table 2. Average values and standard deviation of (i) carbon accumulation in the aerial biomass (CAAB; Mg C ha^{-1}), (ii) biomethane (Nm^3 ha^{-1}), and (iii) bioethanol (L ha^{-1}) yields simulated for the baseline (2000) and 2030 in the marginal areas of Bologna and Catania provinces.

Province	CAAB (Mg C ha^{-1})		Biomethane (Nm^3 ha^{-1})		Bioethanol (L ha^{-1})	
	2000	2030	2000	2030	2000	2030
BO	7.5 ± 1.4	7.4 ± 1.4	5140 ± 955	5098 ± 989	4060 ± 755	4027 ± 781
CT	8.5 ± 1.8	8.6 ± 1.7	5861 ± 1223	5923 ± 1145	4630 ± 966	4679 ± 904

The same considerations are valid for biomethane and bioethanol productions, the former fluctuating around 5118 Nm^3 ha^{-1} in BO and 5892 Nm^3 ha^{-1} in CT, the latter with average values of about 4043 L ha^{-1} in BO and 4654 L ha^{-1} in CT. The maximum simulated values were 6937 Nm^3 ha^{-1} in BO and 9287 Nm^3 ha^{-1} in CT for biomethane and 5480 L ha^{-1} in BO and 7336 L ha^{-1} in CT for bioethanol. In less suitable areas, energy yields dropped below 1200 Nm^3 ha^{-1} for biomethane and 1000 L ha^{-1} for bioethanol, with the lowest values in the province of BO.

The expected trends of potentially attainable energy yields from biomethane, bioethanol, and combustion, under current and future climate in both provinces, are presented in Figure 5.

In agreement with the literature conversion coefficients adopted, energy yields progressively increased moving from bioethanol, to biomethane, and finally to combustible solid, with average values of 91.6, 115.3, and 264 GJ ha^{-1} in BO and 105.5, 132.7, and 303.9 GJ ha^{-1} in CT. Energy gains simulated in CT were always higher than those expected in BO. The distribution of simulated values in CT was always shifted upwards with respect to those projected in BO and the variability connected to combustion yields was about 2.5 times higher than those obtained for other biofuels. Results achieved for biomethane and bioethanol showed very narrow differences in terms of variability regardless of the time frame and province considered. The highest energy performance (479.1 GJ ha^{-1}) was reported by combustible solid at CT in the baseline time frame, whereas the worst results were obtained for bioethanol at CT (12.7 GJ ha^{-1}) and at BO (15.9 GJ ha^{-1}) in 2030. However, when outliers were excluded from analysis, the lowest energy yields simulated in CT for bioethanol were always greater than 50 GJ ha^{-1} in both time frames, i.e., 3.14 times higher than the minimum values obtained in BO.

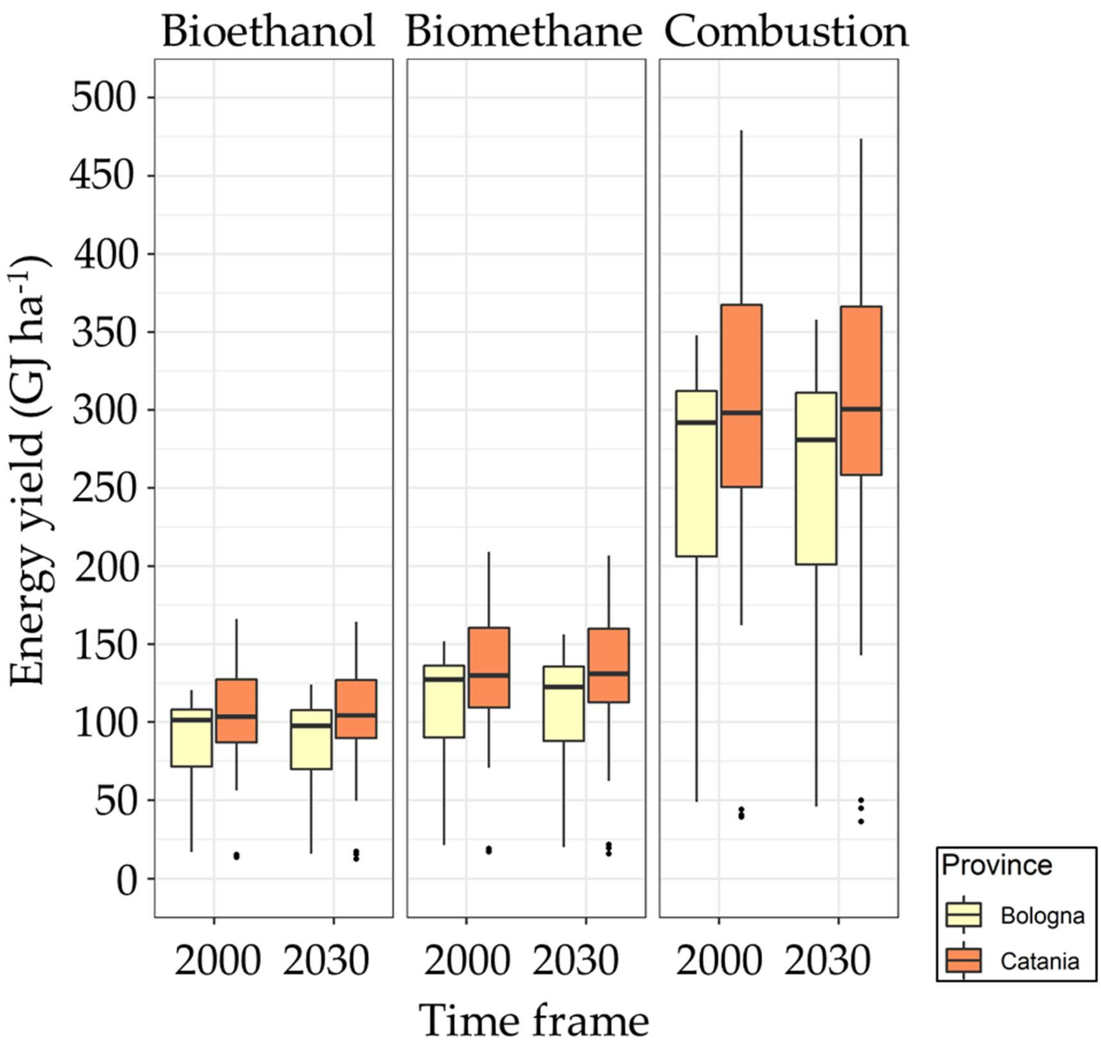

Figure 5. Boxplots of energy yields (GJ ha^{-1}) obtained from simulated (i) bioethanol, (ii) biomethane, and (iii) combustible solid data for the baseline (2000) and 2030 in the marginal areas of Bologna and Catania provinces. Each box derives from the values simulated for the combination year (30) × simulation unit (1226 in Bologna; 4765 in Catania). Black dots represent outliers values.

The spatial representation of achievable energy yields from bioethanol, biomethane, and combustible solid material in CT province is presented in Figure 6, using baseline conditions as input.

The three energy sources showed the same geographical yield pattern across the study area, with highest gains achieved in the central-Western and Southern part of the province and the lowest obtained in the central plain and central-Eastern areas, with a few exceptions. In the best suited marginal areas, energy values reached peaks in the range 80–125 GJ ha^{-1} for bioethanol, 80–175 GJ ha^{-1} for biomethane, and 250–500 GJ ha^{-1} for combustible solid. Less suitable areas presented energy yields between 10 and 80 GJ ha^{-1}, except for combustible solid, which allowed to obtain satisfactory results even in those areas, where pedo-climatic conditions were limiting for crop growing. The areas in the North of the province were considered as not exploitable due to the presence of the Etna volcano.

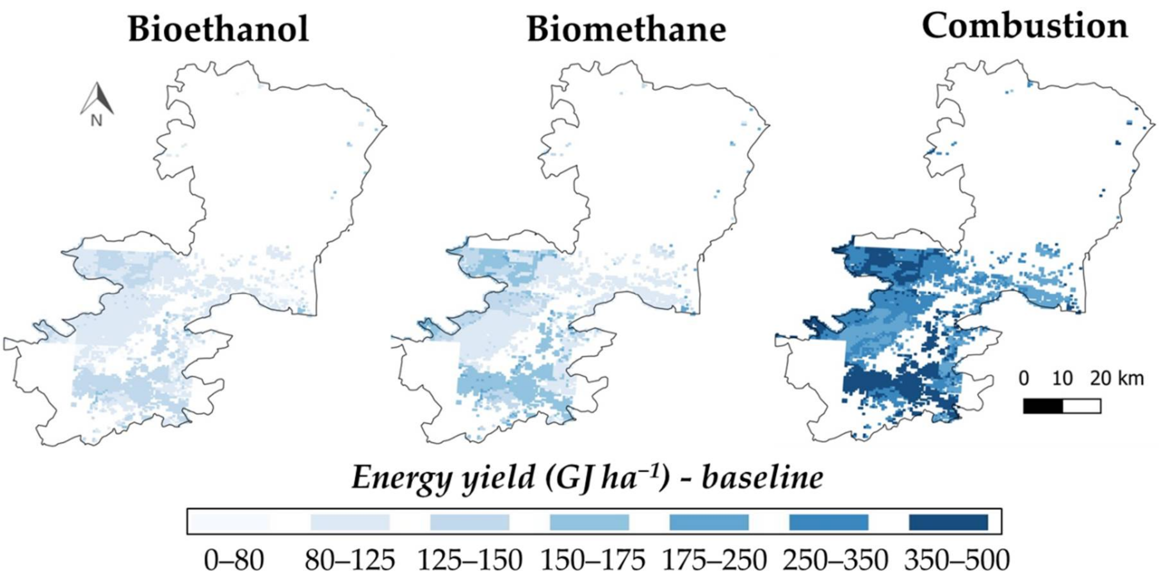

Figure 6. Spatially distributed simulations of energy yield (GJ ha^{-1}) obtainable from different energy sources in the province of Catania under baseline scenario. Results are presented as the average of the values simulated in the whole 30-year period centered on 2000.

The percentage differences in simulated energy yields and natural water consumption between future time frame and baseline are presented as maps in Figure 7.

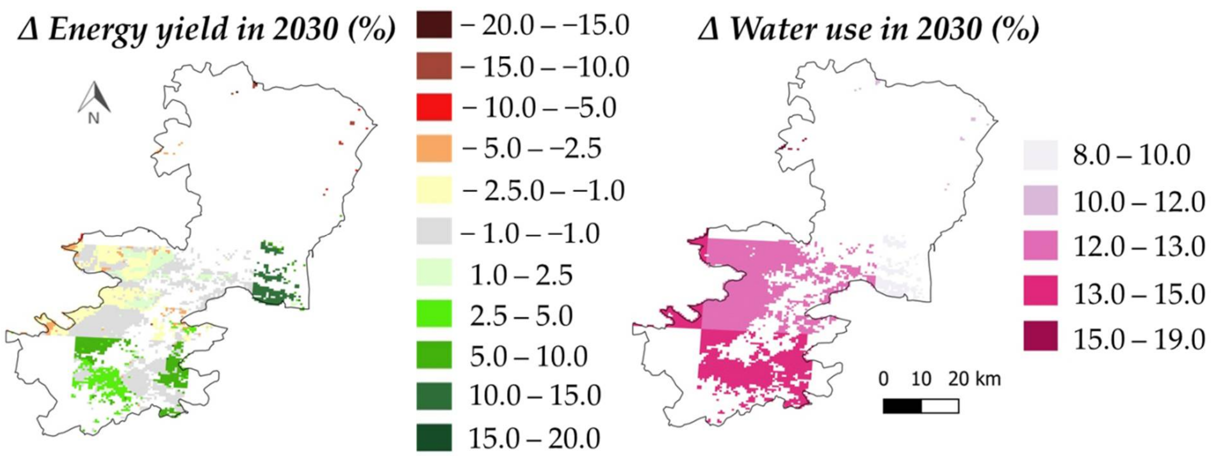

Figure 7. Projected impact of climate change on energy yield and natural water consumption in 2030 in the province of Catania. The results are shown, for each simulation unit, as percentage difference compared to the baseline.

Results showed large heterogeneity across the province, displaying a clear geographic pattern and revealing a predominant role of soil (i.e., texture and depth) versus weather conditions in shaping the spatial variability of simulated energy data across the study area. About 1200 SUs showed positive changes in the range +1/+15%, while approximately 1500 SUs presented relative changes lower than ±1%. Most of the remaining SUs highlighted decreases in terms of energy production ranging from −1 to −5%, suggesting that, in these marginal areas, temperatures were already close to the optimum for the species under current scenario. Among the SUs with high suitability for giant reed in the current scenario, those along the Southern (+2.5–+15%) and Eastern border (up to +20%) showed the largest increases in energy yield, while the areas located in the Western zone reported energy declines in the range of −1 to −5%. The worst results were obtained in the SUs located in the extreme North of the province, where energy yield decreases varied from −15 and −20%. The water use simulated in 2030 time horizon was always higher than in the baseline, with increases represented by a specific geographical pattern: Eastern SUs (+8–+10%) < Northern SUs (+10–+12%) < central SUs (+12–+13%) < Southern and Western SUs (+13–+15%). Peaks in water consumption were observed in the few SUs located in North Western areas of the Catania province.

Under current climate conditions, simulated energy yields presented a very limited variability (Figure 8), with CV values lower than 0.1 in 92% of cases; a larger variability was simulated in the marginal areas along the Eastern border, with CV values up to 15%.

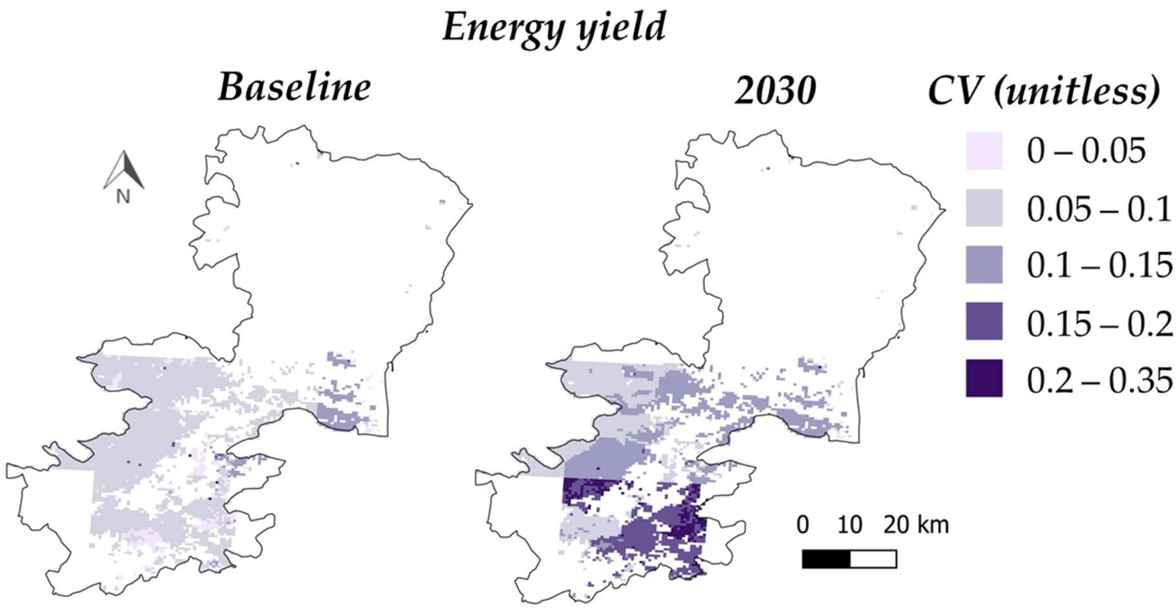

Figure 8. Variability of energy yield simulated across the marginal areas of the Catania province under current and future climate scenarios. The results are presented, for each simulation unit, as coefficient of variation (CV; unitless) computed for the whole 30-year period centered on 2000 (baseline) and 2030 (future climate).

In 2030, the variability of the simulated energy yield is expected to markedly increase throughout the province, with fluctuations around the mean of 10–15% in the central SUs and 20–35% in the Southern SUs; conversely, uncertainty simulated in the Eastern and Western SUs tended to be stationary. All the results presented above, i.e., current productions, natural water consumption, future yield projections, and their stability, should be considered together in order to identify the most promising marginal areas for energy purposes; as a matter of fact, this would increase the chances to fulfill energy plant theoretical demand for biomass, so allowing them to operate close to full capacity.

4. Discussion

4.1. Modelling Perspective

The growing concerns about the projected climate change impact on several energy crops, which are increasing the demand for mid-term analyses on the economic and social sustainability of current production systems. These objectives require the definition of rigorous and transparent procedures dealing with the dynamic simulation of climate change impacts on various sub-domains of cropping systems via spatially explicit application of process-based models. The present study takes steps forward in this direction and, pursuing the approach of adapting models to data, instead of the other way around, can be considered as a shift of paradigm in addressing the problem [64]. The fine spatial resolution and quality of input data used, together with the meticulous approach used to integrate the state-of-the art of crop growth models, IPCC scenarios, and soil databases (i.e., soil physics, hydrology and marginality), allowed to reproduce the high heterogeneity characterizing the systems under study under both boundary and unexplored conditions. Compared to in vivo multi-year and -site open-field trials, model-based simulation experiments are less expensive and time consuming and further allow exploring a larger number of experimental situations. Indeed, Arungro and, more generally, most crop models are capable to reproduce non-linear crop responses to variable pedo-climatic and management conditions, requiring weather and soil input variables commonly stored in agrometeorological databases. In this context, if unavailable, the simulation environment developed allows estimating (i) weather variables (e.g., hourly air temperature, global solar radiation...) based on daily data and/or other weather variables via algorithms included in the CLIMA library [65] and hydrological properties from soil texture and bulk density via pedo-transfer functions [49], respectively coded in dedicated decorators.

The present study differs from previous simulation studies carried out on giant reed via the application of BioMA platform, because it provides a SaaS product instead of releasing an on-premises application, which offers a number of advantages to the user [66]. First, the software is accessible via web without needing to be locally installed in user's PC, so solving long-standing issues related to installation, configuration, and updating. Second, the user always uses the latest and up-to-date version of the application, even if the previous ones are still available, avoiding versioning issues. Third, problems connected to computing capacity are transferred to the service provider, allowing the user to exploit performance and results not achievable by his own device. This also reduces overheads due to the development and management of expensive infrastructure to manage and process data. Fourth, with the same subscription, the customer can use the service from different PC/devices. Fifth, SaaS provides cost-effective infinite scalability opportunities, without requiring users to plan for it. To start, the customer can buy a software for few employees and later decide to adapt it for a larger number of people, after achieving measurable benefits. Sixth, up-to-date security and intrusion detection systems are mandatory infrastructure requirements to provide uninterrupted reliable and safe services. In this context, authorization and security policies ensure that each user's data is kept separate from that of other users.

Climate change impact studies carried out on the same crop in lowlands [27] and wet areas around the river banks [10,28,32] in Northern Italy, provided more optimistic projections compared to those herein presented, because they considered potential growth conditions for water and nutrient availability. As a consequence, relative yield changes expected in the future were always positive, or at most did not show any noticeable change, due to increasingly favorable thermal regimes for this macrothermal species and the absence of possible water stress along crop season, especially in the driest areas. In such conditions, the anticipation of the closed canopy stage and the reduced thermal limitation to photosynthesis simulated under warmer scenarios led to projected gains in productivity, which were not counteracted by higher transpiration rates and decreased water use efficiency. In this context, and on the basis of a more recent study targeting the simulation of giant reed productivity in rainfed conditions in MLs of CT and BO provinces [33], the present analysis focused on the estimation of the attainable energy yield from alternative energy sources (i.e., giant reed-based biomethane, bioethanol, and combustible solid), thus allowing to perform a more complete and informative assessment for farmers and green energy sector stakeholders/researchers, to identify the most promising marginal areas where the Italian bioenergy production can be expanded in a sustainable way.

4.2. Short- and Medium-Term Bioenergy Outlook

The choice of MLs to exploit for energy purposes should primarily be driven by a trade-off between biomass productivity, natural water consumption levels, attainable energy yields, and connected stability under current and future scenarios. Furthermore, regional differences in the state of development of technologies and plants for energy production, presence of medium/long-term projects/investments in the area, road network, and topography should be accounted for. As a matter of fact, it should be considered that economic and environmental costs to cover the distance between production sites and target plant installations significantly affect the sustainability of bioenergy production chain deployment.

In general, the use of combustible solid allows to obtain higher energy yields in both provinces. In this case, the energy conversion of biomass can take place in large-scale thermoelectric plants or in small industrial/domestic plants via direct combustion (after biomass thermal pre-treatment), pyrolysis, and gasification, allowing for different applications (i.e., district heating, power, combined heat and power) [67]. The conversion process presents many advantages: high efficiency (i.e., higher than 90%), reduction of fossil fuels dependence, continuity of energy supply, technological simplicity, cost reduction compared to other renewable energy plants (hydroelectric, thermal, photovoltaic, wind, and geothermal), and reduction of issues related to wastes disposal. Conversely, negative effects concern the emission of carbon monoxide, nitrogen oxides (NOx), volatile organic compounds (VOCs), and particulates, depending on the process, plant and feedstock used. The presence of large-scale, high-efficiency plants in the area is still limited and plant installations supplied or co-supplied by wood biomass are mainly concentrated in the upland areas, where connections with MLs could reveal as a limiting issue. In this context, the production of biomethane can represent a more feasible investment in the short term, given the larger presence of biogas and biomethane plants, especially in the province of BO. Unlike combustion, anaerobic digestion allows for the use of wet biomass and wastes without any pre-treatment [68], and this is crucial since giant reed biomass has a moisture content at harvest of approximately 40–50%, regardless of the crop cutting time. In the case of combustion, an important portion of the energy stored in biomass is dissipated as latent heat of water evaporation, thus reducing the net positive energy balance of this conversion technology even when a pre-drying step is performed. Only the cereal straws harvested in July have a very favorable moisture content of about 10%. Wet biomasses can be used also in the case of bioethanol production, in which heat-based physico-chemical pre-treatments can be optionally applied to promote hemicellulose hydrolysis and the alteration of lignin structure by exposing lignocellulosic materials to high temperature and pressure conditions from several seconds to a few minutes [69]. However, this process proved to be less efficient compared to the other two in terms of energy yield under the explored conditions. Anyhow, biomass chemical pre-treatments—i.e., based on acid, alkali, organic acids, and ionic liquids—can markedly increase biogas, biomethane, bioethanol and, consequently, obtainable energy yields. Despite the study and development of these technologies being recent, they are steadily and rapidly evolving over time, showing a very promising improvement potential in the short term [69]. For this reason, energy yield gains that can be achieved by improving these processes are likely to be substantially higher than those attainable by increasing crop yields via the improvement of agronomy techniques.

Processing plants for bioethanol and biodiesel production and the heat/electrical energy industries are less present in the area, compared to biogas and biomethane installations. Despite the low presence of operative bioenergy plants, the province of Catania emerges as an investment opportunity in the medium and long term, in light of simulation results and given the launch of new projects concerning the installation of new plants involving both the public and private sector. In this context, our simulations revealed a large spatial variability in the performance of giant reed-based systems, thus enabling to identify both critical spots and opportunities for provincial bio-energy sector in current and future time horizons. MLs located in the southern part of the CT province were the best suited areas for bioenergy production as they were characterized by (i) high energy yields in the baseline scenario, (ii) projected energy gains (+5–+10%) in the near future, accompanied by (iii) moderate increases in natural water consumption (+13–+15%). In particular, southern-western MLs stood out as the most suitable since presenting high stability of energy yields, whereas southern-eastern MLs showed a higher yield uncertainty. Central and western MLs appeared the less interesting solutions, the former because it leads to moderate energy production in the current climate with no gains in the future, and the latter because it presents a negative projection for 2030. Finally, MLs located along the eastern border emerged as an interesting investment opportunity, due to the very favorable trade-off between simulated (i) energy yield (increases up to 15–20%), (ii) natural water consumption (raises less than 10%), and stability of the projections in 2030 (CV less than 0.15).

4.3. Final Remarks and Limitations of the Study

The results of this study refer to BO and CT provinces, and inferences can only be made to areas with similar agro-climate, topography, constraints to productivity, and socio-economic characteristics. However, the detail in the information collected to feed the simulation environment allowed to provide plausible projections of energy yield trends in the study areas, considering different conversion processes. Nevertheless, there are some critical points in our approach, mainly connected to the scale of the study, the simulation environment, and prior assumptions.

We did not consider in our simulation any nitrogen stress on crop growth, according to the low giant reed requirements in the study area, as partly demonstrated by negligible yield differences between fertilized and unfertilized giant reed productivity in CT field experiments [37,70]. Indeed, this species is a rhizomatous grass characterized by high mobility of nutrients between above- and belowground organs: In autumn, before harvest, part of nitrogen in aboveground organs is remobilized and stored in the rhizome, and re-used for tiller emission and growth in the next spring re-sprouting [23,71]. Where these assumptions do not hold, hence our results may be slightly overestimated; in such a case, additional data will be needed for model calibration, possibly considering experiments where giant reed biomass is collected under different fertilization strategies. This will also require a further extension of the approaches implemented in the Arungro model to consider the nutrient dynamics and balance in the soil plant system. Unlike in the case of nitrogen, our projections may be partially underestimated because we did not consider the expected positive effects of the increased atmospheric CO_2 concentration on giant reed carbon assimilation rates, mainly due to decreased transpiration, delayed drought responses, and extended periods of assimilation [72]. These effects were not simulated due to the lack of dedicated open-field datasets on the giant reed CO_2 responses in Italian environments, being data published by Nackley et al. [72] limited to closed-topped CO_2 growth chambers conditions. Instead, the lack of algorithms for simulating high temperature-driven limitations to photosynthesis only partially affected simulation results under the explored conditions. Indeed, under both current and future scenarios, temperature rarely exceeded the limiting high temperature identified for giant reed (i.e., 40 °C; Ref. [73]) in the two provinces.

Despite the complex post-harvest processes involved in biomass conversion to energy and their mutual interactions as affected by pre-treatment and process technology that play a key role in determining attainable energy yields, they are not explicitly considered in this study. As a matter of fact, we decided to use empirical conversion coefficients and to focus our analysis on the growing season for three main reasons: (1) pedo-climatic conditions during pre-harvest period play a key role in determining attainable aboveground biomass to feed downstream conversion plants, (2) climate change will affect crop phenology and growth in the future, (3) models for post-harvest conversion (e.g., Ref. [74–76]) require a detailed engineering/process know-how and pertain to a domain that is absolutely independent from the outdoor environment (i.e., do not account for the impact of pedo-climates), and can require a variety of expensive sensors and analytical tools to track system components, measure model parameters, and monitor state variables for model calibration/validation under processing conditions.

In our analysis, we only focused on processes fed with second generation biomasses; next model-based studies may also consider the use of fourth generation substrates, which include genetically engineered, high yielding feedstocks, with low lignin and cellulose contents (thus overcoming concerns deriving from the use of second generation biomasses) [77]. Fourth-generation-based biofuels production technologies could generate beneficial environmental externalities, since they replace fossil fuels with sustainable energy (biofuels) and provide capture/storage of CO_2 emissions along the whole biofuel production process by means, for instance, of oxy-fuel combustion [78]. Despite these technologies still being under development and at experimental stages, they are considered promising to favor carbon-negative rather than carbon-neutral processes [79]. In this case, a comprehensive and informative analysis of the system, quantifying the energy and greenhouse gases (GHGs) balance of biofuels, should require the simulation of GHG emissions associated to the biofuel production, possibly using a supply chain approach. The complexity of this activity depends on the availability of a dedicated module for the simulation of GHG emissions and calibration datasets comprising of multiple in-season measurements of variables related to crop productivity and gas exchanges in the atmosphere-soil-plant system, as well as those connected to biofuel production. The consideration of contrasting experimental environments would further ensure the capability of the simulation engine to reproduce the variability of the production system under study across pedo-climatic conditions. As an alternative, spatial variation in GHG emissions associated with biodiesel production could be performed using simulated Arungro outputs as input into spatial/regional Life Cycle Assessment (LCA) assessment studies (e.g., Ref. [11,80]), in order to identify potential mitigation options for biodiesel production. Our simulation environment could also be seen as an entry point into integrated model-based systems aimed at supporting agro-energy supply chain planning, through a comprehensive evaluation of economic, energy, and environmental sustainability of the supply chain at basin or regional scale [34,81]. In both cases, major criticalities arise from the characterization of the system and related components, and from the collation of reliable input data coherent with the level of detail of the process to be represented.

In this light, our perspective is also to extend the model-based assessment to all the Italian MLs, including the simulation of other energy crops, such as miscanthus (*Miscanthus x giganteus* Greef et Deuter) and/or sweet sorghum (*Sorghum bicolor* L. Moench). In fact, the high heterogeneity of simulation results confirms that our findings cannot be generalized to MLs with different pedo-climatic conditions but rather that the analysis should be carried out locally, looking for site-specific solutions. The simulation of development and growth of other energy crops can be performed by adapting Arungro via parametrization in the case of species characterized by morpho-physiological traits that are similar to those of giant reed; otherwise a different biophysical model should be included in the simulation environment. The decision of which model to use should mainly be driven by a trade-off between the level of detail used to represent the crop and processes under study and the availability of input variables and measured data for calibration/validation. In this context, the modularity of the BioMA architecture allows for an easy (i) model application to other crop/varieties; (ii) implementation of new processes and models; and (iii) refinement of input data resolution, i.e., favoring the development of a system that is more adherent to real conditions. From the SaaS point of view, the implementation of the above-mentioned changes is performed in the system back-end (i.e., the API call remains unchanged) and therefore no software updates are required by the BioMA service user.

5. Conclusions

Few model-based assessments targeting the simulation of the impact of climate change on energy crops productivity and connected attainable bioenergy yield in marginal areas have been performed so far. We focused here on energy yield attainable from giant reed-based biomethane, bioethanol, and combustible solid, considering last generation crop growth models, climate change IPCC scenarios, and databases with high resolution information on Italian soil properties, marginality, and crop suitability to environment.

At the field level, Arungro demonstrated to be able to accurately simulate multiple in-season measurements of carbon accumulation in the aerial biomass under different management and pedo-climates. A slight systematic bias between observed and estimated data was due to delayed rates of biomass accumulation simulated until the peak of tiller population was reached.

At the provincial level, results show an overall stability of giant reed carbon productivity and energy yields over time with large spatial variability between marginal areas, depending on explored weather and soil conditions. Results represented the net balance between the positive effects due to the anticipation of the closed canopy stage and reduced temperature constraints to photosynthesis estimated under warmer scenarios and the negative impacts due to related higher transpiration rates and decreased water use efficiency. The consideration of high-resolution local/provincial-scale heterogeneity and water limitation to crop growth allowed for an in-depth analysis of biomass productivity, natural water consumption, attainable energy yields, and connected stability under current and future scenarios, which finally led to identify critical spots and opportunities within the study area. Furthermore, by analyzing simulation results in relation to the (i) state/prospects of available technologies/plants for energy production in the study area, (ii) the presence of projects/investments for bioenergy plants installation and (iii) the road network/topography makes it possible to define, at both provincial and local scale, the most promising energy sources, the best/less suited marginal areas for giant reed and attainable energy production in the current climate, as well as the investment opportunities in the short and medium/long term.

This exploratory assessment may be extended to other Italian provinces and energy crops (e.g., mischantus poplar and sweet sorghum) and may represent the basis for further studies considering (i) the explicit simulation of energy yield and associated GHG emissions; (ii) the effect of limited nitrogen availability, high temperature stresses and increased atmospheric CO_2 concentration on crop growth; (iii) a full plant and basin scale approach; and (iv) the fourth generation of biofuels production.

Despite the explicit limitations and assumptions, our study provides effective and reliable information on the future trends of giant reed-based energy yield in the short and medium term, which can be of interest for both decision makers and stakeholders of the agricultural sector to expand Italian bioenergy segment in a sustainable way. In this context, the modular approach at the core of the BioMA framework allows for an easy (i) implementation of new biophysical processes, (ii) model application to other crops via model parameterization, and (iii) coupling with a georeferenced database at an optimal spatial resolution. The software was released as a SaaS product, thus allowing the user to run simulations and view the results via a RESTful API call, taking advantage of the high ease of installation, configuration, updating, and accessibility.

Supplementary Materials: The following are available online at https://www.mdpi.com/article/10.3390/land10060548/s1, Text S1: Code documentation of the call to the RESTful API of the Arungro model.

Author Contributions: Conceptualization, G.A.C., F.G. and E.C.; methodology, G.A.C., F.G. and E.C.; software, F.G., D.F. and G.A.C.; formal analysis, G.A.C. and F.G.; investigation, G.A.C. and F.G.; data curation, D.F.; writing—original draft preparation, G.A.C., F.G.; S.A.C.; S.L.C. and E.C.; writing—review and editing, G.A.C., F.G., D.F.; S.A.C.; S.L.C. and E.C.; supervision, G.A.C. All authors have read and agreed to the published version of the manuscript.

Funding: This research was funded by the Italian Ministry of Agriculture (MiPAAF), under the AGROENER project (D.D. n. 26329, 1 April 2016); http://agroener.crea.gov.it/ (accessed on 19 May 2019).

Data Availability Statement: The data presented in this study are available on request from the corresponding author.

Conflicts of Interest: The authors declare no conflict of interest. The funders had no role in the design of the study; in the collection, analyses, or interpretation of data; in the writing of the manuscript, or in the decision to publish the results.

Abbreviations

API	application program interface
AVAL	average value of agricultural land
BioMA	Biophysical Model Applications platform
BO	Bologna
CAAB	carbon accumulation in the aerial biomass
CH_4	methane
CRM	coefficient of residual mass
CT	Catania
CV	coefficient of variation
DM	dry matter
DMI-HIRHAM5-ECHAM5	climate projection generated by HIRHAM5 global circulation model coupled with ECHAM5 regional circulation model
EF	modelling efficiency
EPIC	Environmental Policy Integrated Climate model
ET	evapotranspiration
ETHZ-CLM-HadCM3Q0	climate projection generated by CLM global circulation model coupled with HadCM3Q0 regional circulation model
GHG	greenhouse gas
GIS	geographic information system
HHV	high heating value
IPCC	Intergovernmental Panel on Climate Change
KOH	potassium hydroxide
LHW	lower heating value
METOHC-HadRM3Q0-HadCM3Q0	climate projection generated by HadRM3Q0 global circulation model coupled with HadCM3Q0 regional circulation model
ML	marginal land
MS	modelling solution
NOx	nitrogen oxides
OWS	optimum water supply
R	rainfed
RESTful	representational state transfer
RMSE	root mean square error
RRMSE	relative root mean square error
SaaS	Software as a Service
SMY	specific methane yield
STP	standard temperature and pressure conditions
SU	simulation unit
VOCs	volatile organic compounds
VS	volatile solids

References

1. Jaeger, W.K.; Egelkraut, T.M.M. Biofuel Economics in a Setting of Multiple Objectives & Unintended Consequences. *Renew. Sustain. Energy Rev.* **2011**, *15*, 4320–4333.
2. IRENA. Boosting Biofuels: Sustainable Paths to Greater Energy Security. 2016. Available online: https://www.irena.org/-/media/Files/IRENA/Agency/Publication/2016/IRENA_Boosting_Biofuels_2016.pdf (accessed on 19 May 2021).
3. Searchinger, T.; Heimlich, R.; Houghton, R.A.; Dong, F.; Elobeid, A.; Fabiosa, J.; Tokgoz, S.; Hayes, D.; Yu, T.-H. Use of U.S. croplands for biofuels increases greenhouse gases through emissions from land-use change. *Science* **2008**, *319*, 1238–1240. [CrossRef]
4. Sallustio, L.; Pettenella, D.; Merlini, P.; Romano, R.; Salvati, L.; Marchetti, M.; Corona, P. Assessing the economic marginality of agricultural lands in Italy to support land use planning. *Land Use Policy* **2016**, *76*, 526–534. [CrossRef]
5. Supit, I.; Van Diepen, C.A.; De Wit, A.J.W.; Wolf, J.; Kabat, P.; Baruth, B.; Ludwig, F. Assessing climate change effects on European crop yields using the Crop Growth Monitoring System and a weather generator. *Agric. For. Meteorol.* **2012**, *164*, 96–111. [CrossRef]
6. Donatelli, M.; Srivastava, A.K.; Duveiller, G.; Niemeyer, S.; Fumagalli, D. Climate change impact and potential adaptation strategies under alternate realizations of climate scenarios for three major crops in Europe. *Environ. Res. Lett.* **2015**, *10*, 075005. [CrossRef]

7. Prasad, P.V.; Djanaguiraman, M. Response of floret fertility and individual grain weight of wheat to high temperature stress: Sensitive stages and thresholds for temperature and duration. *Funct. Plant. Biol.* **2014**, *41*, 1261–1269. [CrossRef]
8. Sage, T.L.; Bagha, S.; Lundsgaard-Nielsen, V.; Branch, H.A.; Sultmanis, S.; Sage, R.F. The effect of high temperature stress on male and female reproduction in plants. *Field Crops Res.* **2015**, *182*, 30–42. [CrossRef]
9. Flörke, M.; Schneider, C.; McDonald, R.I. Water competition between cities and agriculture driven by climate change and urban growth. *Nat. Sustain.* **2018**, *1*, 51–58. [CrossRef]
10. Ginaldi, F.; Cappelli, G.A.; Ceotto, E. Modelling-based procedure to evaluate energy crops productivity in marginal humid areas of low po valley (Northern Italy). In Proceedings of the 26th EUBCE European Biomass Conference and Exhibition 2018, Copenhagen, Denmark, 14–17 May 2018; Persson, M., Scarlat, N., Grassi, A., Helm, P., Eds.; ETA-Florence Renewable Energies: Florence, Italy, 2018; pp. 259–262.
11. O'Keeffe, S.; Majer, S.; Drache, C.; Franko, U.; Thrän, D. Modelling biodiesel production within a regional context–A comparison with RED Benchmark. *Renew. Energy* **2017**, *108*, 355–370. [CrossRef]
12. Sołowski, G.; Konkol, I.; Cenian, A. Production of hydrogen and methane from lignocellulose waste by fermentation. A review of chemical pretreatment for enhancing the efficiency of the digestion process. *J. Clean. Prod.* **2020**, *267*, 121721. [CrossRef]
13. Maletta, E.; Díaz-Ambrona, C.H. Lignocellulosic Crops as Sustainable Raw Materials for Bioenergy. In *Green Energy to Sustainability: Strategies for Global Industries*, 1st ed.; Vertès, A.A., Qureshi, N., Blaschek, H.P., Yukawa, H., Eds.; John Wiley & Sons Ltd.: Hoboken, NJ, USA, 2020; pp. 489–514.
14. Liao, J.C.; Mi, L.; Pontrelli, S.; Luo, S. Fuelling the future: Microbial engineering for the production of sustainable biofuels. *Nat. Rev. Microbiol.* **2016**, *14*, 288–304. [CrossRef] [PubMed]
15. Liu, Z.; Wang, K.; Chen, Y.; Tan, T.; Nielsen, J. Third-generation biorefineries as the means to produce fuels and chemicals from CO_2. *Nat. Catal.* **2020**, *3*, 274–288. [CrossRef]
16. Perdue, R.E. Arundo donax—source of musical reeds and industrial cellulose. *Econ. Bot.* **1958**, *12*, 368–404. [CrossRef]
17. Ceotto, E.; Di Candilo, M.; Castelli, F.; Badeck, F.W.; Rizza, F.; Soave, C. Comparing solar radiation interception and use efficiency for the energy crops giant reed (*Arundo donax* L.) and sweet sorghum (*Sorghum bicolor* L. Moench). *Field Crops Res.* **2013**, *149*, 159–166. [CrossRef]
18. Allesina, G.; Pedrazzi, S.; Ginaldi, F.; Cappelli, G.A.; Puglia, M.; Morselli, N.; Tartarini, P. Energy production and carbon sequestration in wet areas of Emilia Romagna region, the role of Arundo Donax. *Adv. Model. Anal. A* **2018**, *55*, 108–113.
19. Lewandosky, I.; Scurlock, J.M.O.; Lindvall, E.; Christou, M. The development and current status of perennial rhizomatous grasses as energy crops in the US and Europe. *Biomass Bioenergy* **2003**, *25*, 335–361. [CrossRef]
20. Webster, R.J.; Driever, S.M.; Kromdijk, J.; McGrath, J.; Leakey, A.D.B.; Siebke, K.; Demetriades-Shah, T.; Bonnage, S.; Peloe, T.; Lawson, T.; et al. High C3 photosynthetic capacity and high intrinsic water use efficiency underlies the high productivity of the bioenergy grass Arundo donax. *Sci Rep.* **2016**, *6*, 20694. [CrossRef] [PubMed]
21. Nocentini, A.; Monti, A. Land-use change from poplar to switchgrass and giant reed increases soil organic carbon. *Agron. Sustain. Dev.* **2017**, *37*, 23. [CrossRef]
22. Ceotto, E.; Castelli, F.; Moschella, A.; Diozzi, M.; Di Candilo, M. Cattle slurry fertilization to giant reed (*Arundo donax* L.): Biomass yield and nitrogen use efficiency. *Bioenergy Res.* **2015**, *8*, 1252–1262. [CrossRef]
23. Ceotto, E.; Marchetti, R.; Castelli, F. Residual soil nitrate as affected by giant reed cultivation and cattle slurry fertilisation. *Ital. J. Agron.* **2018**, *18*, 317–323. [CrossRef]
24. Corno, L.; Pilu, R.; Adani, F. *Arundo donax* L.: A non-food crop for bioenergy and bio-compound production. *Biotechnol. Adv.* **2014**, *32*, 1535–1549. [CrossRef] [PubMed]
25. Ceotto, E.; Vasmara, C.; Marchetti, R.; Cianchetta, S.; Galletti, S. Biomass and methane yield of giant reed (*Arundo donax* L.) as affected by single and double annual harvest. *GCB Bioenergy* **2021**, *13*, 393–407. [CrossRef]
26. Kheshgi, H.S.; Prince, R.C.; Marland, G. The potential of biomass fuels in the context of global climate change: Focus on transportation fuels. *Annu. Rev. Energy Environ.* **2000**, *25*, 199–244. [CrossRef]
27. Cappelli, G.; Yamaç, S.S.; Stella, T.; Francone, C.; Paleari, L.; Negri, M.; Confalonieri, R. Are advantages from the partial replacement of corn with second-generation energy crops undermined by climate change? A case study for giant reed in northern Italy. *Biomass Bioenergy* **2015**, *80*, 85–93. [CrossRef]
28. Vasmara, C.; Cianchetta, S.; Marchetti, R.; Ceotto, E.; Galletti, S. Potassium Hydroxyde Pre-treatment Enhances Methane Yield from Giant Reed (*Arundo donax* L.). *Energies* **2021**, *14*, 630. [CrossRef]
29. Danelli, T.; Sepulcri, A.; Masetti, G.; Colombo, F.; Sangiorgio, S.; Cassani, E.; Anelli, S.; Adani, F.; Pilu, R. *Arundo donax* L. Biomass Production in a Polluted Area: Effects of Two Harvest Timings on Heavy Metals Uptake. *Appl. Sci.* **2021**, *11*, 1147. [CrossRef]
30. Librenti, I.; Ceotto, E.; Di Candilo, M. Biomass characteristics and Energy contents of dedicated lignocellulosic crops. In Proceedings of the Third International Symposium on Energy from Biomass and Waste 2010, Venice, Italy, 8–11 November 2010; CISA, Environmental Sanitary Engineering Centre: Padova, Italy, 2010. 8p. ISBN 978-88-6265-008-3.
31. Ginaldi, F.; Bajocco, S.; Bregaglio, S.; Cappelli, G. Spatializing Crop Models for Sustainable Agriculture. In *Innovations in Sustainable Agriculture*, 1st ed.; Farooq, M., Pisante, M., Eds.; Springer Nature: Cham, Swizerland, 2019; pp. 599–619.

32. Pedrazzi, S.; Allesina, G.; Morselli, N.; Puglia, M.; Barbieri, L.; Lancellotti, I.; Ceotto, E.; Cappelli, G.A.; Ginaldi, F.; Giorgini, L.; et al. The energetic recover of biomass from river maintenance: The rebaf project. In Proceedings of the 25th EUBCE European Biomass Conference and Exhibition 2017, Stockholm, Sweden, 12–15 June 2017; Ek, L., Ehrnrooth, H., Persson, M., Scarlat, N., Grassi, A., Helm, P., Eds.; ETA-Florence Renewable Energies: Florence, Italy, 2017; pp. 52–57.
33. Cappelli, G.A.; Ginaldi, F.; Corinzia, S.A.; Cosentino, S.L.; Fanchini, D.; Ceotto, E. Assessment of giant reed biomass potential (*Arundo donax* L.) in marginal areas of Italy via the application of Arungro simulation model. In Proceedings of the 28th EUBCE European Biomass Conference and Exhibition 2020, Virtual, 6–9 July 2020; Mauguin, P., Scarlat, N., Grassi, A., Helm, P., Eds.; ETA-Florence Renewable Energies: Florence, Italy, 2020; pp. 15–21.
34. Ginaldi, F.; Danuso, F.; Rosa, F.; Rocca, A.; Bashanova, O.; Sossai, E. Agro-energy supply chain planning: A procedure to evaluate economic, energy and environmental sustainability. *Ital. J. Agron.* **2012**, *7*, 221–228. [CrossRef]
35. Stella, T.; Francone, C.; Yamaç, S.S.; Ceotto, E.; Pagani, V.; Pilu, R.; Confalonieri, R. Reimplementation and reuse of the Canegro model: From sugarcane to giant reed. *Comput. Electron. Agric.* **2015**, *113*, 193–202. [CrossRef]
36. Peel, M.C.; Finlayson, B.L.; McMahon, T.A. Updated world map of the Köppen-Geiger climate classification. *Hydrol. Earth Syst. Sci.* **2007**, *11*, 1633–1644. [CrossRef]
37. Cosentino, S.L.; Scordia, D.; Sanzone, E.; Testa, G.; Copani, V. Response of Giant Reed (*Arundo Donax* L.) to Nitrogen Fertilization and Soil Water Availability in Semi-Arid Mediterranean Environment. *Eur. J. Agron.* **2014**, *60*, 22–32. [CrossRef]
38. CREA—Council for Agricultural Research and Economics. *Italian Agriculture in Figures*; CREA—Agricultural Policies and Bioeconomy: Rome, Italy, 2017; p. 183. Available online: https://www.crea.gov.it/documents/68457/0/Itaconta+2017_+ING_DEF_WEB2.pdf/1218e51d-0bf5-03d0-3089-0a56af2e26d5?t=1559117850834 (accessed on 19 May 2021).
39. Battista, F.; Frison, N.; Bolzonella, D. Energy and Nutrients' Recovery in Anaerobic Digestion of Agricultural Biomass: An Italian Perspective for Future Applications. *Energies* **2019**, *12*, 3287. [CrossRef]
40. Susmozas, A.; Martín-Sampedro, R.; Ibarra, D.; Eugenio, M.E.; Iglesias, R.; Manzanares, P.; Moreno, A.D. Process Strategies for the Transition of 1G to Advanced Bioethanol Production. *Processes* **2020**, *8*, 1310. [CrossRef]
41. Williams, J.R.; Jones, C.A.; Kiniry, J.R.; Spanel, D.A. The EPIC crop growth model. *Trans. ASAE* **1989**, *32*, 497–511. [CrossRef]
42. Ritchie, J.T.; Otter, S. Description and performance of CERES-wheat: A user- oriented wheat yield model. In *ARS Wheat Yield Project*; ARS-38; Willis, W.O., Ed.; U.S. Department of Agriculture, Agricultural Research Service: Washington, DC, USA, 1985; pp. 159–175.
43. Scordia, D.; Cosentino, S.L.; Lee, J.W.; Jeffries, T.W. Bioconversion of giant reed (*Arundo donax* L.) hemicellulose hydrolysate to ethanol by Scheffersomyces stipitis CBS6054. *Biomass Bioenergy* **2012**, *39*, 296–305. [CrossRef]
44. Jørgensen, S.E.; Kamp-Nielsen, L.; Christensen, T.; Windolf-Nielsen, J.; Westergaard, B. Validation of a prognosis based upon a eutrophication model. *Ecol. Model.* **1986**, *32*, 165–182. [CrossRef]
45. Loague, K.; Green, R.E. Statistical and graphical methods for evaluating solute transport models: Overview and application. *J. Contam. Hydrol.* **1991**, *7*, 51–73. [CrossRef]
46. Nash, J.E.; Sutcliffe, J.V. River flow forecasting through conceptual models, part I—A discussion of principles. *J. Hydrol.* **1970**, *10*, 282–290. [CrossRef]
47. Moriasi, D.N.; Arnold, J.G.; van Liew, M.W.; Bingner, R.L.; Harmel, R.D.; Veith, T.L. Model evaluation guidelines for systematic quantification of accuracy in watershed simulations. *Trans. ASABE* **2007**, *50*, 885–900. [CrossRef]
48. Duveiller, G.; Donatelli, M.; Fumagalli, D.; Zucchini, A.; Nelson, R.; Baruth, B. A dataset of future daily weather data for crop modelling over Europe derived from climate change scenarios. *Theor. Appl. Climatol.* **2017**, *127*, 573–585. [CrossRef]
49. Wösten, J.H.M.; Lilly, A.; Nemes, A.; Le Bas, C. Development and use of a database of hydraulic properties of European soils. *Geoderma* **1999**, *90*, 169–185. [CrossRef]
50. L'Abate, G.; Fantappie, M.; Priori, S.; D'Avino, L.; Barbetti, R.; Lorenzetti, R.; Costantini, E.A.C. Italian Derived Soil Profile's Database. 1.0. Consiglio per la Ricerca in Agricoltura e L'analisi Dell'economia Agraria (CREA-AA), Online Database. Available online: https://www.crea.gov.it/web/agricoltura-e-ambiente (accessed on 19 May 2021).
51. Sallustio, L.; Harfouche, A.; Marchetti, M.; Salvati, L.; Corona, P. Evaluating the potential of marginal lands available for sustainable cellulosic biofuel production in Italy. *Renew. Sustain. Energy Rev.* **2020**. under review.
52. Ivan, C.; Vasile, R.; Dadarlat, V. Serverless Computing: An Investigation of Deployment Environments for Web APIs. *Computers* **2019**, *8*, 50. [CrossRef]
53. Di Girolamo, G.; Grigatti, M.; Barbanti, L.; Angelidaki, I. Effects of hydrothermal pre-treatments on Giant reed (*Arundo donax*) methane yield. *Bioresour. Technol.* **2013**, *147*, 152–159. [CrossRef] [PubMed]
54. Di Girolamo, G.; Bertin, L.; Capecchi, L.; Ciavatta, C.; Barbanti, L. Mild alkaline pre-treatments loosen fibre structure enhancing methane production from biomass crops and residues. *Biomass Bioenergy* **2014**, *71*, 318–329. [CrossRef]
55. Yang, L.; Li, Y. Anaerobic digestion of giant reed for methane production. *Bioresour. Technol.* **2014**, *171*, 233–239. [CrossRef]
56. Liu, S.; Ge, X.; Liew, L.; Liu, Z.; Li, Y. Effect of urea addition on giant reed ensilage and subsequent methane production by anaerobic digestion. *Bioresour. Technol.* **2015**, *192*, 682–688. [CrossRef]
57. Jiang, D.; Ge, X.; Zhang, Q.; Li, Y. Comparison of liquid hot water and alkaline pretreatments of giant reed for improved enzymatic digestibility and biogas energy production. *Bioresour. Technol.* **2016**, *216*, 60–68. [CrossRef]
58. Shilpi, S.; Lamb, D.; Bolan, N.; Seshadri, B.; Choppala, G.; Naidu, R. Waste to watt: Anaerobic digestion of wastewater irrigated biomass for energy and fertiliser production. *J. Environ. Manag.* **2019**, *239*, 73–83. [CrossRef]

59. Bura, R.; Ewanick, S.; Gustafson, R. Assessment of Arundo donax (giant reed) as feedstock for conversion to ethanol. *Tappi J.* **2012**, *11*, 59–66. [CrossRef]
60. Scordia, D.; Testa, G.; Cosentino, S.L. Perennial grasses as lignocellulosic feedstock for second-generation bioethanol production in Mediterranean environment. *Ital. J. Agron.* **2014**, *9*, 84–92. [CrossRef]
61. Viola, E.; Zimbardi, F.; Valerio, V.; Villone, A. Effect of ripeness and drying process on sugar and ethanol production from giant reed (*Arundo donax* L.). *AIMS. Bioeng.* **2015**, *2*, 29–39. [CrossRef]
62. Angelini, L.G.; Ceccarini, L.; Bonari, E. Biomass yield and energy balance of giant reed (*Arundo Donax* L.) cropped in central Italy as related to different management practices. *Eur. J. Agron.* **2005**, *22*, 375–389. [CrossRef]
63. Bracco, S.; Chinnici, G.; Longhitano, D.; Santeramo, F.G. Prime valutazioni sull'impatto delle produzioni agroenergetiche in Sicilia. *Econ. Dirit. Agroaliment.* **2008**, *3*, 159–192.
64. Ginaldi, F.; Bindi, M.; Marta, A.D.; Ferrise, R.; Orlandini, S.; Danuso, F. Interoperability of Agronomic Long Term Experiment Databases and Crop Model Intercomparison: The Italian Experience. *Eur. J. Agron.* **2016**, *77*, 209–222. [CrossRef]
65. Donatelli, M.; Bellocchi, G.; Carlini, L.; Colauzzi, M. CLIMA: A component-based weather generator. In Proceedings of the MODSIM International Congress on Modelling and Simulation 2005, Melbourne, Australia, 12–15 December 2005; Zerger, A., Argent, R.M., Eds.; Modelling and Simulation Society of Australia and New Zealand: Melbourne, Australia, 2005; pp. 627–633.
66. Ju, J.; Ya, W.; Fu, J.; Wu, J.; Lin, Z. Research on Key Technology in SaaS. In Proceedings of the IEEE 2010 International Conference on Intelligent Computing and Cognitive Informatics, Kuala Lumpur, Malaysia, 22–23 June 2010; pp. 384–387.
67. Caillat, S.; Vakkilainen, E. 9—Large-Scale Biomass Combustion Plants: An Overview. In *Biomass Combustion Science, Technology and Engineering*; Woodhead Publishing Series in Energy; Rosendahl, L., Ed.; Woodhead Publishing: Sawston, UK; Cambridge, UK, 2013; pp. 189–224.
68. Appels, L.; Lauwers, J.; Degrève, J.; Helsen, L.; Lievens, B.; Willems, K.; Van Impe, J.; Dewil, R. Anaerobic digestion in global bio-energy production: Potential and research challenges. *Renew. Sustain. Energy Rev.* **2011**, *15*, 4295–4301. [CrossRef]
69. Menon, V.; Rao, M. Trends in bioconversion of lignocellulose: Biofuels, platform chemicals & biorefinery concept. *Prog. Energy Combust. Sci.* **2012**, *38*, 522–550.
70. Cosentino, S.L.; Patanè, C.; Sanzone, E.; Testa, G.; Scordia, D. Leaf Gas Exchange, Water Status and Radiation Use Efficiency of Giant Reed (*Arundo Donax* L.) in a Changing Soil Nitrogen Fertilization and Soil Water Availability in a Semi-Arid Mediterranean Area. *Eur. J. Agron.* **2016**, *72*, 56–69. [CrossRef]
71. Di Nasso, N.N.; Roncucci, N.; Bonari, E. Seasonal dynamics of aboveground and belowground biomass and nutrient accumulation and remobilization in giant reed (*Arundo donax* L.): A three-year study on marginal land. *BioEnergy Res.* **2013**, *6*, 725–736. [CrossRef]
72. Nackley, L.L.; Vogt, K.A.; Kim, S.H. Arundo donax water use and photosynthetic responses to drought and elevated CO_2. *Agric. Water Manag.* **2014**, *136*, 13–22. [CrossRef]
73. Barney, J.N.; DiTomaso, J.M. Global climate niche estimates for bioenergy crops and invasive species of agronomic origin: Potential problems and opportunities. *PLoS ONE* **2011**, *6*, e17222. [CrossRef]
74. Batstone, D.J.; Puyol, D.; Flores-Alsina, X.; Rodríguez, J. Mathematical modelling of anaerobic digestion processes: Applications and future needs. *Rev. Environ. Sci. Bio/Technol.* **2015**, *14*, 595–613. [CrossRef]
75. Nosrati-Ghods, N.; Harrison, S.T.L.; Isafiade, A.J.; Tai, S.L. Mathematical Modelling of Bioethanol Fermentation From Glucose, Xylose or Their Combination—A Review. *ChemBioEng Rev.* **2020**, *7*, 68–88. [CrossRef]
76. Gabriel, K.J.; El-Halwagi, M.M. Modeling and optimization of a bioethanol production facility. *Clean Technol. Environ.* **2013**, *15*, 931–944. [CrossRef]
77. Dutta, K.; Daverey, A.; Lin, J.-G. Evolution retrospective for alternative fuels: First to fourth generation. *Renew. Energy* **2014**, *69*, 114–122. [CrossRef]
78. Oh, Y.K.; Hwang, K.-R.; Kim, C.; Kim, J.R.; Lee, J.-S. Recent developments and key barriers to advanced biofuels: A short review. *Bioresour. Technol.* **2018**, *257*, 320–333. [CrossRef]
79. Ziolkowska, J.R. Biofuels technologies: An overview of feedstocks, processes, and technologies. In *Biofuels for a More Sustainable Future: Life Cycle Sustainability Assessment and Multi-Criteria Decision Making*, 1st ed.; Ren, J., Scipioni, A., Manzardo, A., Liang, H., Eds.; Elsevier B.V.: Amsterdam, The Netherlands, 2020; pp. 1–19.
80. O'Keeffe, S.; Thrän, D. Energy crops in regional biogas systems: An integrative spatial LCA to assess the influence of crop mix and location on cultivation GHG emissions. *Sustainability* **2020**, *12*, 237. [CrossRef]
81. Lee, M.; Cho, S.; Kim, J. A comprehensive model for design and analysis of bioethanol production and supply strategies from lignocellulosic biomass. *Renew. Energy* **2017**, *112*, 247–259. [CrossRef]